
PERGAMON

Journal of Quantitative Spectroscopy & Radiative Transfer 68 (2001) 689–735

Journal of Quantitative Spectroscopy & Radiative Transfer

www.elsevier.com/locate/jqsrt

A linearized discrete ordinate radiative transfer model for atmospheric remote-sensing retrieval

R.J.D. Spurr*, T.P. Kurosu, K.V. Chance

Harvard-Smithsonian Center for Astrophysics, 60 Garden Street, Cambridge, MA 02138, USA

Received 25 August 1999; accepted 19 May 2000

Abstract

The radiative transfer forward model simulation of intensities and associated parameter derivatives (weighting functions) is a vital part of the retrieval of earth atmospheric constituent information from measurements of backscattered light. The discrete ordinate method is the most commonly used approach for the determination of solutions to the radiative transfer equation. In this paper, we carry out an internal perturbation analysis of the complete discrete ordinate solution in a plane parallel multi-layered multiple-scattering atmosphere. Perturbations in layer atmospheric quantities will translate into small changes in the single-scatter albedos and optical depth values. In addition, we consider perturbations in layer thermal emission source terms and in the surface albedo. It is shown that the solution of the boundary value problem for the perturbed intensity field leads in a natural way to the weighting function associated with the parameter causing the perturbation. We have developed a numerical model LIDORT (linearized discrete ordinate radiative transfer) for the simultaneous generation of backscatter intensities and weighting function output at arbitrary elevation angles, for a user-defined set of atmospheric variations. Results for a 5-layer test atmosphere with two scatterers and thermal emission terms are shown. Intensities are validated against benchmark discrete ordinate results, while weighting functions are checked for consistency against finite difference results based on external perturbations. A second example is presented for a 60-layer terrestrial atmosphere with molecular and aerosol scattering and ozone trace gas absorption in the UV spectral range; weighting functions are shown to correspond closely with results derived from another radiative transfer model. Published by Elsevier Science Ltd.

* Corresponding author.

0022-4073/01/$ - see front matter. Published by Elsevier Science Ltd.
PII: S0022-4073(00)00055-8

1. Introduction

1.1. Background and rationale

The derivation of atmospheric constituent distributions and surface properties from surface-based, airborne and satellite remote-sensing instruments plays a vital role in monitoring the earth's atmosphere and understanding the chemical and physical processes therein. A common feature of all retrievals is the need for an accurate forward model for the generation of synthetic quantities such as radiances, fluxes and weighting functions. The model should include a full treatment of all orders of scattering. Accurate multiple-scatter forward models are also critical for addressing problems in stellar and planetary atmospheres.

The retrieval process will generate estimates of a number of atmospheric parameter distributions which together constitute the *state vector* $\mathbf{X}$ of parameters to be retrieved. The retrieval is the formal inverse of the forward problem $\mathbf{Y} = F(\mathbf{X})$, where $\mathbf{Y}$ is the vector of synthetic measurements and F is a function describing the attenuation of solar and/or thermal emission radiation in the atmosphere by means of absorption, scattering and reflection of light. This function is specified by a radiative transfer model. In most cases, F has a complex dependence on the atmospheric parameters $\mathbf{X}$, and the inverse problem is often solved with a non-linear iterative scheme based on likelihood estimation. Uncertainties in the retrieval will depend not only on the accuracy of the instrumental measurements but also on uncertainties inherent in the modeling of the atmosphere and on assumptions made about the accuracy of any a priori information.

Non-linear least-squares fitting [1] has been and continues to be a standard technique for many remote-sensing problems, for example the global fitting of limb emission spectra [2]. The optimal estimation retrieval algorithm [3,4] has found much use in constituent profile retrieval from backscatter and emission measurements. In particular, we note the application of this method to ozone profile retrieval from nadir backscatter measurements made by instruments such as SBUV [5] and GOME [6–8]. A number of related retrieval techniques are used in the remote sensing context, including Phillips–Tikhonov regularization [9], and Chahine inversion [10]. In order to illustrate the retrieval requirement for forward model synthetic measurements and associated weighting functions, we give an example for the optimal estimation approach [3,4].

The solution of the inverse problem $\mathbf{X} = F^{-1}(\mathbf{Y})$ is constrained by the existence of an independent a priori state vector $\mathbf{X}_a$ with error covariance $\mathbf{S}_a$. Assuming Gaussian statistics with error covariance $\mathbf{S}_m$ associated with measurement vector $\mathbf{Y}_m$, the optimization minimizes with respect to $\mathbf{X}$ the functional

$$\Phi = (X - X_a)^{\mathrm{T}} S_a^{-1} (X - X_a) + (Y - F(X))^{\mathrm{T}} S_m^{-1} (Y - F(X)). \tag{1}$$

The T-superscript denotes matrix transpose. If the forward model is linearized about the state $\mathbf{X}_n$:

$$F(X) = F(X_n) + K_n(X - X_n) + \mathcal{O}(X - X_n)^2, \tag{2}$$

then the estimate for the next guess of the state vector is given by

$$X_{n+1} = X_a + G^{-1} K_n^{\mathrm{T}} S_m^{-1} [(Y_{\mathrm{meas}} - Y_n) - K_n(X_a - X_n)], \tag{3}$$

where

$$G = K_n^{\mathrm{T}} S_m^{-1} K_n + S_a^{-1}. \tag{4}$$

Here, $\mathbf{Y}_n = F(\mathbf{X}_n)$ is the synthetic measurement computed from a forward model calculation based on atmospheric state vector $\mathbf{X}_n$, and $\mathbf{K}_n$ is the Jacobean matrix of forward model parameter derivatives (also known as weighting functions) evaluated at $\mathbf{X}_n$. $\mathbf{K}_n$ represents the responses of the simulated intensity to small changes in atmospheric parameters that make up state vector $\mathbf{X}_n$. (Henceforth we use the term "weighting functions" for $\mathbf{K}_n$). The starting point for the state vector iteration is often taken to be the a priori value. For optimal estimation and other iterative retrieval algorithms, it is clear that the radiative transfer model must generate the set $\{\mathbf{Y}_n, \mathbf{K}_n\}$ for each state vector estimate $\mathbf{X}_n$.

In many circumstances, a simplified model of atmospheric light attenuation can be used, for which weighting functions can be determined in a straightforward manner from explicit expressions. Thus for example in solar occultation viewing, extinction of the line-of-sight solar beam predominates over atmospheric backscatter, which is ignored in the forward model (see for example [10] for SAGE II retrieval). However for instruments measuring backscattered light in the UV, visible and near-infrared regions, multiple scattering of light in the earth's atmosphere is an important physical process that cannot be neglected. Although accurate values for $\mathbf{Y}_n$ for multiple scattering scenarios have been determined from a variety of radiative transfer (RT) solution methods (see [11] for a summary of techniques), less attention has been paid to the calculation of weighting functions $\mathbf{K}_n$.

Finite difference approximations to $\mathbf{K}_n$ have often been derived by using *external* perturbations. Here, two independent simulations of the atmospheric attenuation are made, one for an unperturbed atmosphere, the other for an atmosphere in which a single parameter has been changed by a small amount; the intensities are subtracted and divided by the parameter change. This process must be repeated for each parameter to be retrieved, and at every iteration step of the retrieval. In addition to the time-consuming nature of this approach, the accuracy depends in a rather ad hoc manner on the magnitude of the external perturbation. This is particularly evident when the optical properties depend in a complex non-linear fashion on the atmospheric parameter in question (for example, temperature).

The main purpose of this paper is the development of a forward model LIDORT (Linearized Discrete Ordinate Radiative Transfer) that will generate quickly and accurately any desired set of backscatter weighting functions in a multi-layered atmosphere with anisotropic scatterers, as well as the backscatter intensity field. The model is based on the discrete ordinate method for the solution of the radiative transfer equation (RTE). This method has a long history, from the pioneering work of Chandrasekhar in the 1940s [12,13] to the DISORT package developed by Stamnes and co-workers in the 1980s [14]. DISORT in particular has been widely used in atmospheric radiative transfer applications, and has recently been installed in MODTRAN [15] to provide a reliable scattering formalism.

The discrete ordinate approach uses optical depth as the vertical coordinate; scattering properties are specified by means of layer single-scatter albedos and phase functions. The method reduces the full RTE to a set of coupled *linear* first-order differential equations. We show that first-order perturbation analysis may be carried out explicitly on the discrete ordinate solutions to these equations. Furthermore, we show that the boundary condition problem applied to the *perturbed* intensity field generates in a natural way the complete field of first-order parameter derivatives. Analytic expressions may be developed for all weighting functions, which can then be calculated rapidly and to the same level of accuracy as the (unperturbed) backscattered intensity.

We look at the following general scenario pertinent to satellite retrieval applications in the earth's atmosphere. We confine our attention to intensity and weighting function output for upwelling radiation at the top of the atmosphere (TOA). The atmosphere will be assumed plane-parallel, with each layer treated as homogeneous and possessing several non-conservative scattering particulates. Two sources of light will be considered — the beam source (prototype for solar illumination) and an isotropic thermal emission source. No diffuse light is incident on the top of the atmosphere. The atmosphere is bounded below by a reflecting surface with a known bi-directional or Lambertian reflection function. The lower boundary may also have a thermal emission property (assumed isotropic). The scope of the plane-parallel DISORT package [14] covers this scenario, and this version of DISORT will be used as the standard for validating the backscatter intensity results. Polarization effects are not included.

For weighting function derivation, we need to know how variations in layer atmospheric quantities will be manifested as changes to the layer single-scatter albedos and optical thickness values. We will not consider changes to phase function angular distributions (although this is in principle possible in the perturbation analysis). The effect of atmospheric parameter variations will also be included in the thermal emission source term. For the surface property, we will consider perturbations of the total surface albedo (but not the angular distribution of the bi-directional reflectance) and the surface emission term. These assumptions will allow a wide variety of weighting functions to be derived, including those with respect to layer trace gas concentrations, layer temperatures and pressures, cloud and aerosol scattering and extinction coefficients, molecular scattering coefficients, and thermal emission coefficients.

As part of the algorithm development for the GOME satellite instrument [16], a weighting function analysis has been carried out on the GOMETRAN RT model developed for this instrument [17]. This model uses altitude rather than optical depth as the vertical coordinate, and the RTE for a multi-layered atmosphere is solved using finite differences for the altitude derivatives. This transforms the complete problem to a linear matrix algebra system [18,19], which is then subject to first-order perturbation theory for the generation of weighting function output. As is often the case with altitude finite-differencing, great care must be taken with the choice of vertical grid. This version of GOMETRAN has been used in some studies of ozone profile retrieval from GOME nadir backscatter measurements using optimal estimation methods [7,8].

1.2. Overview of the paper

In Section 2 we recapitulate the discrete ordinate solution for the backscattered intensity. Following the basic RTE definitions (Section 2.1), the description falls into two parts: (1) solution of the discrete ordinate differential equations for the homogeneous and particular integrals for each layer, the component solutions being evaluated at the computational quadrature angles (Section 2.2); (2) the intensity field derivation using appropriate boundary conditions at the top and bottom of the atmosphere, plus continuity of the field at intermediate layer boundaries, to fix the constants of integration; the solution is completed using the *post-processing function*, that is, the derivation of intensities for arbitrary (user-defined) zenith angles using the source function integration method (Section 2.3). This exposition follows closely the DISORT description [14]. Although much of this material is familiar (see for example [14] or [20]), the exposition given here is designed to illuminate the perturbation analysis that follows.

In Section 3.1 we introduce some definitions and rules for the first-order perturbation analysis of the discrete ordinate solution. In Section 3.2 we apply these rules to the layer homogeneous and particular solutions of the perturbed RTE. This is followed by a description of the boundary conditions required for the perturbed intensity field (Section 3.3). Section 3.4 outlines the derivation of analytic expressions for TOA weighting functions with respect to layer parameters for both the discrete ordinate stream angles and the post-processed off-quadrature directions; the TOA albedo weighting functions are treated in Section 3.5. The whole of Section 3 is designed to give an overall summary and description of the weighting function analysis without going into excessive mathematical detail. Most of the algebraic manipulations have been placed in Appendices A–C.

An analytic formulation of the discrete ordinate solution for a single layer was first developed by Chandrasekhar [12,13] using the full-space quadrature scheme over the interval $(-1, 1)$. It turns out that a complete analytic perturbation analysis can also be developed with this quadrature scheme. This approach is not as flexible or as powerful as the "double" quadrature eigenproblem method used in DISORT and the present work. The original Chandrasekhar solution and the corresponding perturbation analysis are presented for completeness in Appendix D.

In Section 4 we consider the numerical model LIDORT developed from the theory in Sections 2 and 3, and provide two examples of weighting function simulations. Following some discussion of the model and its implementation (Sections 4.1–4.3), the first example treats a 5-layer atmosphere with two scatterers and beam and thermal source terms; this scenario will illustrate the principles behind the weighting function derivations. In Section 4.5, we examine a realistic scenario involving a 60-layer terrestrial atmosphere with both molecular (Rayleigh) and aerosol scattering, and including ozone absorption, for a number of wavelengths in the UV region. In both examples, we check the LIDORT weighting function output by comparing with external finite-difference values obtained from independently calculated intensities based on perturbed atmospheric parameters. In addition, values of intensity in all cases are checked against DISORT results for the same scenarios. Finally, we show that the weighting function results in Section 4.5 are consistent with values computed from the GOMETRAN model [17] for the same scenario.

In Section 5 following the summary, we remark on future developments for LIDORT. These include (i) additional options to output weighting function fields at arbitrary optical depths and stream angles, for both upwelling and downwelling directions; (ii) the generation of mean-value output (fluxes, mean intensities); (iii) the treatment of the direct beam attenuation in a curved atmosphere; and (iv) a vectorization of the model for the treatment of fully polarized light. The first three developments have been carried out, and will be the subject of a second paper (R. Spurr, in preparation).

2. The discrete ordinate solution

2.1. *Radiative transfer equation* (*RTE*)

The equation of radiative transfer for the diffuse intensity field I in a plane-parallel scattering medium may be written as

$$\mu \frac{\mathrm{d}I(\tau, \mu, \phi)}{\mathrm{d}\tau} = I(\tau, \mu, \phi) - J(\tau, \mu, \phi). \tag{5}$$

The scattering is assumed to be completely coherent (no redistribution among wavelengths), so that Eq. (5) is valid for a monochromatic intensity field. The optical depth coordinate τ is measured perpendicular to the medium boundaries with $\tau = 0$ at TOA, and the direction is specified through μ (absolute value of the cosine of the zenith angle) and ϕ (azimuth angle). In this paper, the source term J is defined to be

$$J(\tau,\mu,\phi) = J_{\text{ext}}(\tau,\mu,\phi) + \frac{\omega(\tau)}{4\pi}\int_0^{2\pi} \mathrm{d}\phi' \int_0^1 \mathrm{d}\mu' P(\tau,\mu,\phi;\mu',\phi')I(\tau,\mu',\phi'). \tag{6}$$

Here $J_{\text{ext}} = J_{\text{beam}} + J_{\text{thermal}}$ is the sum of the beam and atmospheric thermal emission source terms, $\omega(\tau)$ is the single-scatter albedo, and $P(\tau,\mu,\phi;\mu',\phi')$ the phase function; the last term in Eq. (6) represents the multiple scatter contribution.

The source term J_{beam} corresponds to scattering of a parallel beam of incident flux $\mu_0 F_\odot$ in direction $\{-\mu_0,\phi_0\}$; J_{thermal} represents thermal emission (assumed isotropic) as determined by a Planck function $B(T)$ at temperature T (which is regarded as a function of τ). Specifically:

$$J_{\text{beam}}(\tau,\mu,\phi) = \frac{F_\odot}{4\pi}\,\omega(\tau)P(\tau,\mu,\phi;-\mu_0,\phi_0)\mathrm{e}^{-\tau/\mu_0}, \tag{7}$$

$$J_{\text{thermal}}(\tau,\mu,\phi) = (1-\omega(\tau))B(T). \tag{8}$$

Next, we expand the intensity as a Fourier cosine series in the relative azimuth $\phi_0 - \phi$, and the phase function as a series of Legendre polynomials in the cosine of the scatter angle Θ between directions $\{\mu,\phi\}$ and $\{\mu',\phi'\}$:

$$I(\tau,\mu,\phi) = \sum_{m=0}^{2N-1} I^m(\tau,\mu)\cos m(\phi_0-\phi), \tag{9}$$

$$P(\cos\Theta) = \sum_{l=0}^{2N-1} \beta_l P_l(\cos\Theta), \tag{10}$$

where β_l are the phase function moments of the Legendre expansion, and

$$\cos\Theta = \mu\mu' + \sqrt{(1-\mu^2)(1-\mu'^2)}\cos(\phi-\phi'). \tag{11}$$

This development yields a separate equation for each of the $2N$ Fourier components

$$\mu\frac{\mathrm{d}I^m(\tau,\mu)}{\mathrm{d}\tau} = I^m(\tau,\mu) - \int_{-1}^{1} D^m(\tau,\mu,\mu')I^m(\tau,\mu')\,\mathrm{d}\mu' - J^m_{\text{ext}}(\tau,\mu), \tag{12}$$

where $m = 0,1,\ldots,2N-1$. The external source term may be written as

$$J^m_{\text{ext}}(\tau,\mu) = \delta_{0m}(1-\omega(\tau))\sum_{s=0}^{S} b_s\tau^s + \frac{F_\odot}{2\pi}\,\mathrm{e}^{-\tau/\mu_0}(2-\delta_{m0})D^m(\tau,\mu,\mu_0). \tag{13}$$

The auxiliary quantities $D^m(\tau,\mu,v)$ are defined by

$$D^m(\tau,\mu,v)=\frac{\omega(\tau)}{2}\sum_{l=m}^{2N-1}\beta_l(\tau)P_l^m(\mu)P_l^m(v). \tag{14}$$

The $P_l^m(\mu)$ are associated Legendre polynomials. The addition theorem for Legendre polynomials has been used in the Fourier decomposition. For the thermal source term, the Planck function $B(T)$ has been expressed as a power series in optical depth [21], where the b_s are the expansion coefficients.

In the Nth discrete ordinate approximation, the multiple scatter source term integral is replaced by a quadrature sum defined by the set $\{\mu_i,a_i\}$, $i=(\pm 1,\ldots,\pm N)$ of Gauss–Legendre quadrature abscissae and weights. In order to obtain RTE solutions, the atmosphere is assumed to consist of a number of homogeneous layers, with ω and β_l constant for a given layer. In the rest of this section we confine our attention to one such layer (the superposition of layers will be addressed in Section 2.3). The solution for Fourier component m is then determined by solving the set of $2N$ linear first-order differential equations for $I^m(\mu_i)$, the intensities at the computational (quadrature) stream angles

$$\mu_i\frac{\mathrm{d}I^m(\tau,\mu_i)}{\mathrm{d}\tau}=I^m(\tau,\mu_i)-\sum_j a_jD^m(\tau,\mu_i,\mu_j)I^m(\tau,\mu_j)-J^m_{\mathrm{ext}}(\tau,\mu_i). \tag{15}$$

Here, $j=(\pm 1,\ldots,\pm N)$ is the quadrature sum. In this equation, $J^m_{\mathrm{ext}}(\tau,\mu_i)$ and $D^m(\tau,\mu_i,\mu_j)$ are given by Eqs. (13) and (14) evaluated at the quadrature cosines.

Two kinds of quadrature regimes are usual — a full-range ("single") scheme over the interval $(-1,1)$, and a "double" scheme with quadratures defined separately for $\mu\in(0,1)$ and $\mu\in(-1,0)$. In both cases $\mu_{-j}=\mu_j$ and $a_{-j}=a_j$, for $j=1,\ldots,N$. For the single scheme, the abscissae are just the $2N$ zeros of $P_{2N-1}(\mu)$ in the interval $(-1,1)$. The single scheme was used by Chandrasekhar in his original development of an analytic discrete ordinate solution to Eq. (15) (see Appendix D); this solution depends on the orthonormality of the Legendre polynomial set $\{P_l(\mu),l=0,1,\ldots,2N-1\}$.

The double quadrature scheme reflects in a natural way the upward and downward stream separation of the intensity field, and the symmetrical distribution of abscissae about $\mu=\pm 0.5$ ensures a more representative spread of points around $\mu=0$ and $|\mu|=1$ than that achieved with the single scheme. With the advent of an eigenvalue approach to the solution of Eq. (15), the double scheme has now become standard in DISORT (see [20] and references therein for a discussion of quadratures). The double scheme is adopted as the default in the present work, though the option to use the single scheme and the analytic solution developed in Appendix D has been retained in the numerical model.

2.1.1. Surface boundary condition

The lower surface of the atmosphere is assumed to have a general bi-directional reflecting property. The bi-directional surface reflection function $\rho(\mu,\phi;\mu',\phi')$ is expanded as a Fourier series in cosine azimuth

$$\rho(\mu,\phi;\mu',\phi')=\rho_0(\mu,\mu')+2\sum_{m=1}^{2N-1}\rho_m(\mu,\mu')\cos m(\phi-\phi'). \tag{16}$$

In the discrete ordinate approximation, the reflection condition for the mth Fourier component of the diffuse intensity at the lower boundary is then

$$I^m(+\mu_i) = (1+\delta_{m0})\sum_{j=1}^{N} \mu_j a_j I^m(-\mu_j)\rho_m(\mu_i,-\mu_j), \quad \text{where } i=1,\ldots,N. \tag{17}$$

In the present work, a normalized form of the bi-directional reflection is used:

$$\rho_m(\mu_i,-\mu_j) = R\rho_m^*(\mu_i,-\mu_j), \quad \text{where } R = \frac{1}{4}\int_0^1\int_0^1 \mu\mu'\rho_0(\mu,\mu')\,\mathrm{d}\mu\,\mathrm{d}\mu'. \tag{18}$$

R is the surface albedo. For the Lambertian case, $\rho_0^*(\mu_i,\mu_j)=1$ for all streams and $\rho_m^*=0$ for $m>0$. Expressions for ρ_m may be derived from invariance principles [12], and these functions have been investigated in a number of applications ranging from planetary atmospheres [22] to the treatment of terrestrial clouds as bi-directional reflecting surfaces [23].

The upwelling radiation at the lower boundary $\tau=\tau_g$ also has a contribution from the reflection of the direct beam; this has the form

$$I^m_{\text{direct}}(\mu_i,\tau_g) = \frac{F_\odot\mu_0}{\pi}\,\mathrm{e}^{-\tau_g/\mu_0}R\rho_m^*(\mu_i,-\mu_0). \tag{19}$$

Furthermore, for the azimuth-independent component, a surface emission term may be included:

$$I_{\text{emission}}(\mu_i) = \delta_{m0}\kappa(\mu_i)B(T_g), \tag{20}$$

where the black-body function $B(T_g)$ depends on surface temperature T_g. The directional surface emissivity $\kappa(\mu)$ is determined from Kirchhoff's law

$$\kappa(\mu) = 1 - 2R\int_0^1 \mu'\rho_0^*(\mu,\mu')\,\mathrm{d}\mu'. \tag{21}$$

2.2. Solutions of the basic equations

2.2.1. Homogeneous solution

We summarize the main results from the eigenvalue approach to the homogeneous RTE developed by Stamnes and co-workers [14,21,24]. The treatment is the same for each Fourier component, and we henceforth drop the index m except where necessary (for example in the Legendre sum in Eq. (23) below). Homogeneous solutions of (15) may be found with the ansatz $I_j \propto X_j\exp(-k\tau)$ for $j=\pm1,\ldots,\pm N$. Because of the quadrature symmetry, it can be shown that the values of k^2 are real numbers satisfying the following reduced eigenvalue equation of order N:

$$(\Gamma - k^2E)\varsigma = 0 \quad \text{where } \Gamma = (\zeta-\eta)(\zeta+\eta). \tag{22}$$

With indices $i,j=1,\ldots,N$, the matrices ζ and η are given by

$$\zeta_{ij} = (D^+_{ij}a_j - \delta_{ij})/\mu_i \quad \text{and} \quad \eta_{ij} = D^-_{ij}a_j/\mu_i \quad \text{with } D^\pm_{ij} = \frac{\omega}{2}\sum_{l=m}^{2N-1}\beta_l P^m_l(\mu_i)P^m_l(\pm\mu_j). \tag{23}$$

In the above, E is the unit matrix. Values of k occur in pairs $\pm k_\alpha$, $\alpha=1,\ldots,N$. The corresponding solution vectors are $X^\pm_{j\alpha}$, and these are related to the eigenvectors ς of Eq. (22) by means of the

relation $\varsigma_{j\alpha} = X^+_{j\alpha} + X^-_{j\alpha}$. The difference vector defined by $\vartheta_{j\alpha} = X^+_{j\alpha} - X^-_{j\alpha}$ satisfies the following auxiliary equation linking it to the eigenvector ς:

$$k_\alpha \vartheta_{i\alpha} = \sum_{j=1}^{N} (\zeta_{ij} + \eta_{ij})\varsigma_{j\alpha}. \tag{24}$$

Details of these derivations may be found in [14,21]. For components of $X^\pm_{j\alpha}$ at negative stream angles, we use the symmetry relations

$$X^+_{-j\alpha} = X^-_{j\alpha} \quad \text{and} \quad X^-_{-j\alpha} = X^+_{j\alpha}. \tag{25}$$

The eigenproblem in Eq. (22) can be solved reliably using standard numerical packages such as those in LAPACK [25]. A suitable LAPACK driver would be module DGEEV (double precision) for a general non-symmetric eigenmatrix such as Γ in (22). However, DGEEV looks for real and imaginary components, and it is quicker to use a dedicated routine solving for real eigenvalues only. The module ASMYTX as used in DISORT is convenient for this purpose. Both modules are implemented in the code; DGEEV and ASYMTX give identical results in all cases, but the latter is faster. A normalization condition will be imposed on the eigenvectors (this will be important in the perturbation analysis):

$$\|\varsigma^2_\alpha\| \equiv \sum_{j=1}^{N} \varsigma^2_{j\alpha} = 1 \quad \text{for } \alpha = 1, \ldots, N. \tag{26}$$

Eigenvectors from the ASYMTX module are unnormalized; those from DGEEV already satisfy (26).

2.2.2. Particular solutions

For the particular solution of (15) appropriate to the plane-parallel beam source term, an ansatz of the form $I_j \sim W_j \exp(-\tau/\mu_0)$ yields the following (see [21] for details):

$$\sum_{j=-N}^{N} A^{(\text{beam})}_{ij} W_j = B^{(\text{beam})}_i, \tag{27}$$

where

$$A^{(\text{beam})}_{ij} = \left(1 + \frac{\mu_i}{\mu_0}\right)\delta_{ij} - a_j D_{ij} \quad \text{and} \quad B^{(\text{beam})}_i = \frac{F_\odot}{2\pi}(2 - \delta_{m0})D(\mu_i, -\mu_0). \tag{28}$$

D_{ij} is defined as in (23), but with indices $i, j = \pm 1, \ldots, \pm N$ for all stream angles. $D(\mu_i, -\mu_0)$ is defined similarly for the cosine of the beam solution zenith angle. Eq. (27) may be solved as a standard linear matrix algebra problem for the component values W_j. In the model, this is done using the LAPACK combination DGETRF for an LU-factorization of the matrix $A^{(\text{beam})}$, followed by DGETRS for the solution by backsubstitution. Note that it is possible to use the intrinsic symmetry of the discrete ordinate equations to halve the order of system (27); one then requires an auxiliary equation and sum and difference vectors defined in a similar way to those used for the homogeneous solution (see for example [26]).

The particular solution of Eq. (15) corresponding to the thermal emission source term may be found with the power-series substitution $I_j = \delta_{m0} \sum_{s=0}^{S} T_{j,s}\tau^s$. Successive powers of optical depth

τ in the resulting polynomial are equated to zero, generating the following recurrence relation for the coefficients $T_{j,s}$:

$$\sum_j A_{ij}^{(\text{thermal})} T_{j,s} = \begin{cases} (1-\omega) b_s e_i & \text{for } s = S, \\ (1-\omega) b_s e_i + (s+1)\mu_i T_{i,s+1} & \text{for } s < S, \end{cases} \tag{29}$$

where $A_{ij}^{(\text{thermal})} = \delta_{ij} - a_j D_{ij}$ and e_i is a $2N$-vector with unit entries. The linear algebra system in (29) can again be solved using LAPACK modules DGETRF for the LU-decomposition of $A^{(\text{thermal})}$, followed by repeated application of DGETRS for the recurrence coefficients $T_{j,s}$.

2.3. Boundary conditions and the complete solution

We assume there are K homogeneous layers in the atmosphere, with $K+1$ layer boundaries. We use indices p, q and r for labeling layers. Combining the discrete ordinate homogeneous solutions and the particular integrals, the *quadrature* components of the diffuse intensity in layer p are given by

$$I_{jp} = \sum_{\alpha=1}^{N} L_{p\alpha} X_{jp\alpha}^{+} \mathrm{e}^{-k_{p\alpha}(\tau - \tau_{p-1})} + M_{p\alpha} X_{jp\alpha}^{-} \mathrm{e}^{-k_{p\alpha}(\tau_p - \tau)} + J_{jp}, \tag{30}$$

where

$$J_{jp} = W_{jp} \exp(-\tau/\mu_0) + \delta_{m0} \sum_{s=0}^{S} T_{jp,s} \tau^s. \tag{31}$$

Suitable boundary conditions will enable the integration constants $L_{p\alpha}$ and $M_{p\alpha}$ to be determined. Here we have used the scaling transformation suggested by Stamnes and Conklin [24] and used in DISORT [14] to ensure that the exponential factors remain bounded and the discrete ordinate solution numerically stable. The boundary conditions are (see Fig. 1a):

(BC1) no downward diffuse radiation at the top of atmosphere;
(BC2) continuity of the intensity field at all intermediate levels;
(BC3) a surface reflection condition at the lowest level.

In terms of the discrete ordinate solutions (30), these conditions may be written, respectively, as

$$I_{-jp}(\tau_0) = 0 \quad \text{for } j = 1, \ldots, N \text{ and } p = 1, \tag{32a}$$

$$I_{jr}(\tau_r) = I_{jp}(\tau_r) \quad \text{for } j = \pm 1, \ldots, \pm N \text{ and } 1 < p \le K,\ r = p-1, \tag{32b}$$

$$I_{jK}(\tau_K) = (1+\delta_{m0}) R \sum_{i=1}^{N} a_i \mu_i \rho_m^*(\mu_j, -\mu_i) I_{-iK}(\tau_K) + I^*(\mu_j) \quad \text{for } j = 1, \ldots, N. \tag{32c}$$

Here, $I^*(\mu_j)$ in (32c) comprises a surface emission term and a reflection of the direct beam:

$$I^*(\mu_j) = \delta_{m0} \kappa(\mu_j) B(T_g) + \frac{F_\odot \mu_0}{\pi} \mathrm{e}^{-\tau_K/\mu_0} R \rho_m^*(\mu_j, -\mu_0). \tag{33}$$

Defining transmittance factors $\Theta_{p\alpha} = \exp(-k_{p\alpha}\Delta_p)$, for $p = 1, \ldots, K$ and $\alpha = 1, \ldots, N$, where $\Delta_p = (\tau_p - \tau_{p-1})$ is the optical thickness of layer p, we substitute the discrete ordinate solutions (30)

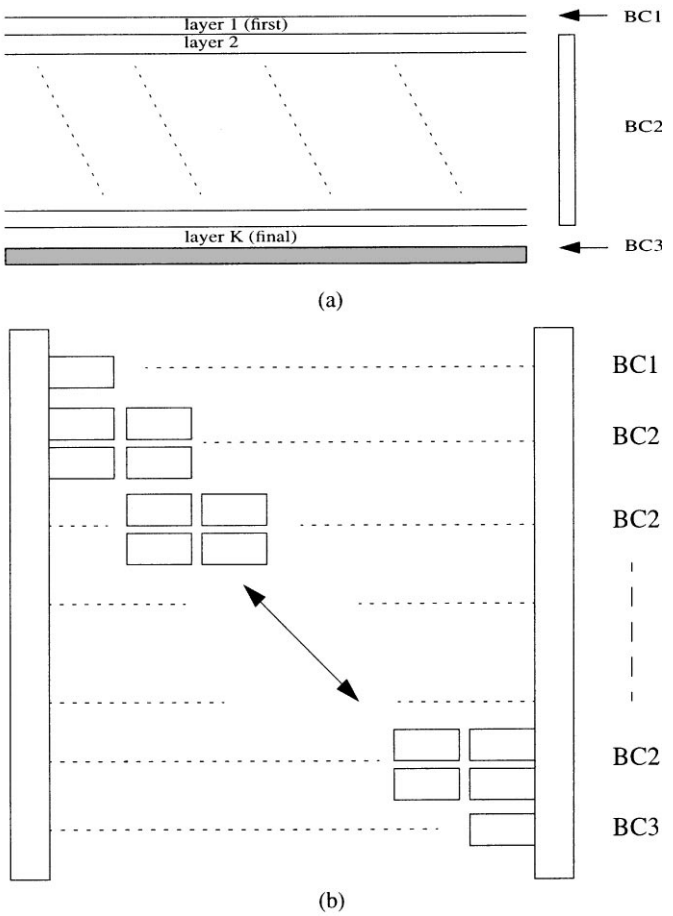

Fig. 1. (a) Boundary conditions for the discrete ordinate solution in a multi-layer atmosphere; (b) schematic matrix structure for the boundary value problem. All marked blocks have N rows and $2N$ columns, with K layers in total; the matrix has $2NK$ columns and $2NK$ rows, with $3N-1$ sub- and super-diagonals. All other entries are zero.

into the boundary conditions (32a)–(32c) to arrive at the following set of equations which define the linear algebra system for the solution of the boundary value problem:

$$\sum_{\alpha=1}^{N} \{L_{p\alpha} X^{+}_{-jp\alpha} + M_{p\alpha}\Theta_{p\alpha} X^{-}_{-jp\alpha}\} = -J_{-jp}\Big|_{\tau_0}, \tag{34a}$$

$$\sum_{\alpha=1}^{N} [\{L_{r\alpha}\Theta_{r\alpha} X^{+}_{jr\alpha} + M_{r\alpha} X^{-}_{jr\alpha}\} - \{L_{p\alpha} X^{+}_{jp\alpha} + M_{p\alpha}\Theta_{p\alpha} X^{-}_{jp\alpha}\}] = (J_{jp} - J_{jr})\Big|_{\tau_r}, \tag{34b}$$

$$\sum_{\alpha=1}^{N} \{L_{p\alpha}\Theta_{p\alpha}\Phi^{+}_{j\alpha} + M_{p\alpha}\Phi^{-}_{j\alpha}\} = I^{*}(\mu_j) - \Psi_j\Big|_{\tau_K}. \tag{34c}$$

Eq. (34a) is BC1 for $p=1$ and $j=1,\ldots,N$; (34b) is BC2 for $p=2,\ldots,N$, $r=p-1$ and $j=\pm 1,\ldots,\pm N$; and (34c) is BC3 for $p=K$ and $j=1,\ldots,N$. J_{jp} are the particular integrals

evaluated at the optical depths indicated. We have the following two auxiliary equations for the BC3 condition:

$$\Phi_{j\alpha}^{\pm} = X_{jK\alpha}^{\pm} - (1+\delta_{m0})R\sum_{i=1}^{N} a_i\mu_i\rho_m^*(\mu_j,-\mu_i)X_{iK\alpha}^{\pm}, \tag{35a}$$

$$\Psi_j = J_{jK}\Big|_{\tau_K} - (1+\delta_{m0})R\sum_{i=1}^{N} a_i\mu_i\rho_m^*(\mu_j,-\mu_i)J_{-iK}\Big|_{\tau_K}. \tag{35b}$$

Eqs. (34a)–(34c) may be written in the matrix form $\mathscr{A}\mathscr{X} = \mathscr{B}$, and solved simultaneously for the vector $\mathscr{X}$ of unknowns. The structure of the matrix $\mathscr{A}$ is shown in Fig. 1b; the order of this linear system is $2NK$. The matrix $\mathscr{A}$ has $3N-1$ sub- and super-diagonals; once it is compressed into band-storage form, a standard LU-decomposition linear matrix algebra package can be used to find the solution efficiently. To this end, the double-precision driver modules DGBTRF and DGBTRS from LAPACK [25] were used. DBGTRF executes the LU-factorization of $\mathscr{A}$ and is called once. DGBTRS finds the solution $\mathscr{X}$ by backsubstitution and can be called repeatedly for different vectors $\mathscr{B}$. In particular, it will be seen in Section 3 that the weighting function problem reduces in essence to the creation of a series of vectors $\mathscr{B}_c$ which depend on the parameter c being varied; the matrix $\mathscr{A}$ is unchanged.

The above procedure gives the intensity field at the *quadrature* streams for any optical depth in the atmosphere, and for a single Fourier component. For the satellite application, the upwelling TOA intensity field may be found by substituting $\tau = 0$ for $p = 1$ and $j = 1,\ldots,N$ in (30).

For the intensity at arbitrary μ, we use the source function integration technique (also known as "post-processing") which was first developed by Chandrasekhar [12], and is now standard practice in discrete ordinate theory. It has been shown (see for example [20]) that in addition to preserving continuity at off-quadrature stream cosines, this method is superior to numerical interpolation over the quadrature solutions. Here we confine our attention to upwelling TOA intensity.

The procedure relies on the formal integration of Eq. (5). In an inhomogeneous atmosphere, source terms must be integrated on a layer-by-layer basis. We adopt the recurrence relation

$$I_{p-1}(\mu) = I_p(\mu)\gamma_p(\mu) + \Lambda_p(\mu) \tag{36}$$

for the upwelling intensity $I_{p-1}(\mu)$ at the top of layer p. The layer transmittance factor is defined to be $\gamma_p(\mu) = \exp(-\Delta_p/\mu)$ where $\Delta_p = \tau_p - \tau_{p-1}$, and the *integrated layer source term* Λ_p is defined by

$$\Lambda_p(\mu) = \int_{\tau_{p-1}}^{\tau_p} \frac{\mathrm{d}\tau}{\mu} J_p(\tau,\mu)\mathrm{e}^{-(\tau-\tau_{p-1})/\mu}. \tag{37}$$

The recurrence is valid for $p = K, K-1,\ldots,1$. The starting value is the bottom-of-the-atmosphere source term $I_K(\tau_K,\mu)$, and the desired TOA result is $I_0(\mu)$. In (37), the term $J_p(\tau,\mu)$ in the integrand is approximated by its discrete ordinate form

$$J_p(\tau,\mu) \simeq \frac{F_\odot}{2\pi}(2-\delta_{m0})D(\mu,-\mu_0)\mathrm{e}^{-\tau/\mu} + \sum_j a_j D(\mu,\mu_j)I_p(\tau,\mu_j), \tag{38}$$

where the $D(\mu,\mu_j)$ and $D(\mu,-\mu_0)$ terms are defined as before, but with the arbitrary stream cosine μ replacing the quadrature values μ_i. One can then perform the optical depth integrations explicitly

and write down closed-form expressions for the layer source terms and the recursion starter $I_K(\tau_K, \mu)$. For the details of these calculations, refer to Appendix C.

This completes the solution for a single Fourier component; to generate the intensity field at arbitrary azimuth angles, we sum these components according to Eq. (9). Although it is possible to compute all Fourier terms ($2N - 1$ harmonics require at least N half-space quadratures), it is usual to terminate the azimuth series when the addition of an extra harmonic does not alter the overall intensity by more than a pre-specified relative amount υ (a typical value is $\upsilon = 0.005$). This convergence test must be satisfied for each output stream. Furthermore, it makes sense to apply this convergence test to at least two successive azimuth contributions to avoid accidental omissions (the Rayleigh scatter intensity contribution for $m = 2$ is greater than that for $m = 1$ for example). This procedure is adopted in the present work, in line with the policy of DISORT [14] and GOMETRAN [19] regarding series convergence.

3. Perturbation analysis of the discrete ordinate solution

3.1. Rules for the layer perturbation analysis

For a multi-layer atmosphere, we wish to determine the sensitivity of the discrete ordinate solution to a variation in a single atmospheric variable x_q defined in layer q. A perturbation in x_q will induce changes in the main optical inputs for the layer, namely the single-scatter albedo ω_q and the layer optical thickness Δ_q. We suppose that x_q changes by a relative amount ε, and that to first order in ε, this induces a *relative* change of $u_q\varepsilon$ in ω_q, and an *absolute* change of $v_q\varepsilon$ in Δ_q. The variation x_q in layer q does not affect single-scatter albedos in other layers. However, the optical depth value at the bottom of the layer q has increased by $v_q\varepsilon$; for all layers below q, the optical depth values are increased by the same amount. The quantities u_q and v_q depend on the constitution and physical properties of the atmosphere. Since the discrete ordinate method is a generic *scattering formalism*, it is not necessary to know this dependence in the perturbation analysis that follows. Using primes to denote first-order perturbed values, we write

$$x'_q = x_q(1 + \varepsilon), \tag{39a}$$

$$\omega'_p = \begin{cases} \omega_q(1 + u_q\varepsilon) & \text{for } p = q, \\ \omega_p & \text{otherwise,} \end{cases} \tag{39b}$$

$$\tau'_p = \begin{cases} \tau_p + v_q\varepsilon & \text{for } p \geq q, \\ \tau_p & \text{for } p < q. \end{cases} \tag{39c}$$

To include sensitivity to the thermal emission source term, we suppose that the variable x_q induces an absolute change h_{qs} in each of the Planck function coefficients b_{qs} in Eq. (13); coefficients for layers other than q are not affected. Thus

$$b'_{ps} = \begin{cases} b_{ps} + \varepsilon h_{ps} & \text{for } p = q,\ s = 0, \ldots, S, \\ b_{ps} & \text{otherwise.} \end{cases} \tag{39d}$$

These are the *perturbation analysis rules*. The variational quantities u_q, v_q and h_{qs} are inputs to the model; the examples in Section 4 will illustrate the construction of these inputs for two test-case atmospheres. It should be noted that the above rules apply only to plane-parallel atmospheres; for a curved-atmosphere treatment of the direct beam attenuation (the "pseudo-spherical" model), the rules governing the optical depth variation v_q are quite different (R. Spurr, paper in preparation).

3.2. Perturbation analysis of the discrete ordinate component solutions

Now we examine the discrete ordinate solution given by (30) and (31). For layer q, the beam source particular solution vector W_{jq} and the eigenvalues $k_{q\alpha}$ and solution vectors $X_{jq\alpha}$ of the homogeneous equation depend only on the single-scatter albedo ω_q for that layer. In fact, all three of these quantities are directly proportional to ω_q, and it follows from (39b) that changes in these quantities are directly proportional to $u_q\varepsilon$. The first-order perturbed values of k, X and W are thus defined as

$$k'_{q\alpha} = k_{q\alpha} + u_q\varepsilon f_{q\alpha}, \tag{40a}$$

$$X'_{jq\alpha} = X_{jq\alpha} + u_q\varepsilon Y_{jq\alpha}, \tag{40b}$$

$$W'_{q\alpha} = W_{q\alpha} + u_q\varepsilon Z_{q\alpha}. \tag{40c}$$

The thermal emission particular solution vector T_{jqs} depends both on ω_q and on the expansion coefficients b_{qs}. For this term the first-order perturbed value is defined to be

$$T'_{jqs} = T_{jqs} + \varepsilon V_{jqs}. \tag{40d}$$

In these definitions, $j = \pm 1, \ldots, \pm N$ labels the quadrature streams, $\alpha = 1, \ldots, N$ labels the eigensolutions, and $s = 0, \ldots, S$ labels the thermal expansion coefficients. These definitions apply only to the RTE solutions in layer q; for other layers, unperturbed values of the homogeneous solution and particular integrals may be used.

The first task of the perturbation analysis is to establish the quantities f, Y, Z and V defined in Eqs. (40a)–(40d). To derive f and Y, it is necessary to construct a perturbed form of the eigenproblem (22) based on the single-scatter albedo variation u_q; the normalization condition (26) provides an additional constraint. First-order theory reduces the calculation to a linear algebra system of order $N + 1$. The details of this calculation can be found in Appendix A. Perturbation analysis for the particular integral factors Z and V is more straightforward, since the *original* (unperturbed) solution vectors W and T were determined through linear matrix algebra; the details are also given in Appendix A.

Assuming these component factors have been determined, we move on to the second stage of the analysis.

3.3. Perturbation analysis of the boundary value problem

This is the most important step of the analysis. We require perturbed values of the constants of integration, which we define as follows:

$$L'_{p\alpha} = L_{p\alpha} + \varepsilon N_{p\alpha}, \tag{41a}$$

$$M'_{p\alpha} = M_{p\alpha} + \varepsilon P_{p\alpha}. \tag{41b}$$

These definitions are valid for all layers $p = 1, \ldots, K$ and for $\alpha = 1, \ldots, N$. The task of this section is to determine the factors $N_{p\alpha}$ and $P_{p\alpha}$.

We can write down expressions for the perturbed intensity field I'_{jp}, making a distinction between layer q in which varying atmospheric property x_q induces changes in both single-scatter albedo and optical depth, layers $p < q$ for which there is no change in optical depth, and layers $p > q$, for which only the optical depths are altered. Specifically:

$$I'_{jp} = W'_{jp}\mathrm{e}^{-\tau/\mu_0} + \sum_{\alpha=1}^{N} L'_{p\alpha}X'^{+}_{jp\alpha}\mathrm{e}^{-k'_{p\alpha}(\tau-\tau_r)} + M'_{p\alpha}X'^{-}_{jp\alpha}\mathrm{e}^{-k'_{p\alpha}(\tau'_p-\tau)} \quad \text{for } p = q, \tag{42a}$$

$$I'_{jp} = W_{jp}\mathrm{e}^{-\tau/\mu_0} + \sum_{\alpha=1}^{N} L'_{p\alpha}X^{+}_{jp\alpha}\mathrm{e}^{-k_{p\alpha}(\tau-\tau_r)} + M'_{p\alpha}X^{-}_{jp\alpha}\mathrm{e}^{-k_{p\alpha}(\tau_p-\tau)} \quad \text{for } p < q, \tag{42b}$$

$$I'_{jp} = W_{jp}\mathrm{e}^{-\tau/\mu_0} + \sum_{\alpha=1}^{N} L'_{p\alpha}X^{+}_{jp\alpha}\mathrm{e}^{-k_{p\alpha}(\tau-\tau'_r)} + M'_{p\alpha}X^{-}_{jp\alpha}\mathrm{e}^{-k_{p\alpha}(\tau'_p-\tau)} \quad \text{for } p > q. \tag{42c}$$

Only the beam source term has been included in the above (this is purely for convenience of exposition). In these definitions, $\tau'_p = \tau_p + \varepsilon v_q$ for $p \geq q$, $r = p - 1$, and the argument τ is regarded as a dummy variable.

The key point is that the *same boundary conditions hold for the perturbed field* as those applied to the original field. There are three cases to be distinguished and eight separate conditions; these are illustrated in Fig. 2, and summarized below with reference to the set of equations (42a)–(42c). The general situation involves variation in a layer q that is somewhere in the middle of the atmosphere (Case 1, BCL1–BCL6). For $q = 1$, we have Case 2 with modified TOA condition BCL3M followed by BCL4 to BCL6. For Case 3, $q = K$ (bottom layer), and we require BCL1 to BCL3 followed by a modified lower boundary condition BCL4M. The eight conditions are:

(BCL1) No downward diffuse radiation for $p = 1$ at $\tau = \tau_0$.
$\Rightarrow$ Set Eq. (42b) to zero for downwelling streams;
(BCL2) Continuity at level $\tau = \tau_{p-1}$, for $1 < p < q$.
$\Rightarrow$ Equate two expressions of type (42b) at this level, for all streams;
(BCL3) Continuity at upper boundary $\tau = \tau_{q-1}$ of layer q.
$\Rightarrow$ Equate (42a) and (42b) at this level, for all streams;
(BCL4) Continuity at lower boundary $\tau = \tau_q$ of layer q.
$\Rightarrow$ Equate (42a) and (42c) at this level, for all streams;
(BCL5) Continuity at level $\tau = \tau_p$, for $q < p < K$.
$\Rightarrow$ Equate two expressions of type (42c) at this level, for all streams;
(BCL6) Surface boundary condition for $p = K$ at $\tau = \tau_K$.
$\Rightarrow$ Construct condition from expressions of type (42c) at this level;
(BCL3M) No downward diffuse radiation for $q = 1$ at $\tau = \tau_0$.
$\Rightarrow$ Set Eq. (42a) to zero for downwelling streams;
(BCL4M) Surface boundary condition for $q = K$ at $\tau = \tau_K$.
$\Rightarrow$ Construct condition from expressions of type (42a) at this level.

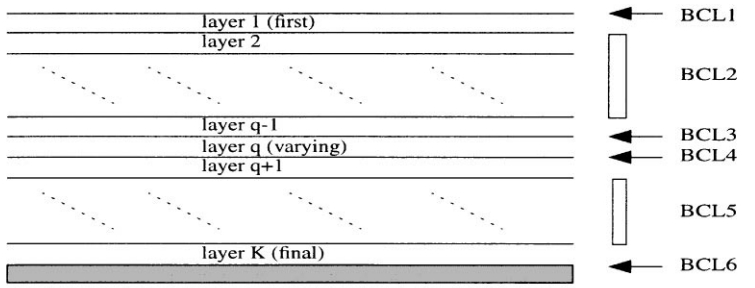

Case 1: 1 < q < K (varying layer in middle of atmosphere).

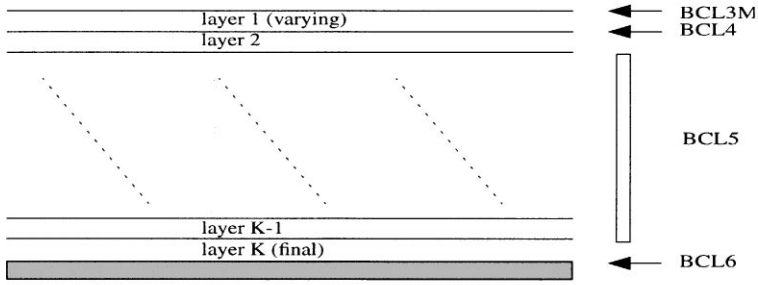

Case 2: q = 1 (varying layer at top of atmosphere).

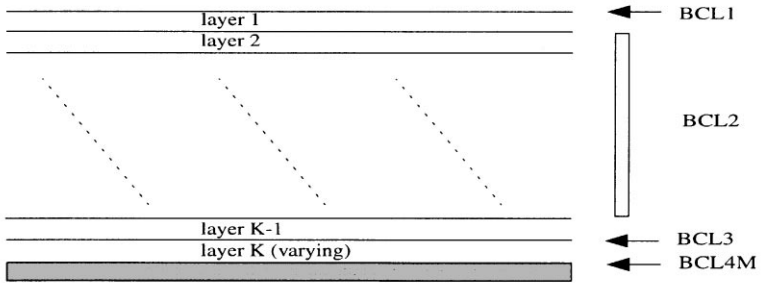

Case 3: q = K (varying layer at bottom of atmosphere).

Fig. 2. Boundary conditions for the perturbed discrete ordinate solution in a multilayer atmosphere.

Explicit analytic expressions for these eight boundary conditions can be found in Appendix B. It is seen that the boundary value solution for $N_{p\alpha}$ and $P_{p\alpha}$ has the *same form* as that used in Section 2.3 for constants $L_{p\alpha}$ and $M_{p\alpha}$. Recalling the linear system $\mathscr{A}\mathscr{X} = \mathscr{B}$ defined by conditions BC1, BC2 and BC3 for the original field, we now have a similar system $\mathscr{A}\mathscr{X}^* = \mathscr{B}^*$ for the perturbed boundary conditions. Here, the column vector $\mathscr{B}^*$ depends uniquely through u_q and v_q on the atmospheric parameter x_q that is being varied, and of course on the layer q in which the variation occurs. Since the matrix $\mathscr{A}$ has been established and its LU-decomposition already performed for the unperturbed boundary value problem, it follows that solutions $\mathscr{X}^*$ may be found

by straightforward backsubstitution using the LU-factorized form of $\mathscr{A}$. Thus the determination of the perturbed integration constants is equivalent to the construction of a series of column vectors $\mathscr{B}^*$ for each parameter to be varied. These column vectors may be constructed from the detailed expressions listed in Appendix B.

3.4. Layer weighting function computation

We now have all the ingredients in place for an explicit derivation of the complete discrete ordinate solution for the perturbed field corresponding to a variation x_q in layer q. The *normalized weighting function components* for the quadrature streams μ_j are found by relaxing the first-order perturbation

$$\mathscr{K}_{jp}(x_q) = x_q \frac{\partial I_{jp}}{\partial x_q} = \lim_{\varepsilon \to 0} \frac{I'_{jp} - I_{jp}}{\varepsilon}. \tag{43}$$

This definition is quite general and weighting functions for the quadrature streams can be computed at any optical depth. For the TOA upwelling values, set $p = 1$ and $\tau = 0$. To determine the perturbed field (and hence the weighting functions) at TOA for arbitrary zenith angles μ, we must carry out a post-processing evaluation of the perturbed field. We may write down a perturbed version of the recursion relation (36)

$$I'_{p-1}(\mu) = I'_p(\mu)\gamma'_p(\mu) + \Lambda'_p(\mu). \tag{44}$$

Note that $\gamma'_q(\mu) = \gamma_q(\mu)(1 - v_q\varepsilon/\mu)$, and $\gamma'_p(\mu) = \gamma_p$ since only layer q contributes to the variation of optical thickness Δ_q. To determine $\Lambda'_p(\mu)$, we go back to the original expressions derived in Appendix C.1 using the source function integration method, and apply the perturbations explicitly using the quantities derived in Sections 3.2 and 3.3 for the perturbed discrete ordinate solution. This is a relatively involved exercise, and care must be taken to distinguish between the layer q containing the varying parameter x_q and all other layers. We also require the perturbed bottom-of-the-atmosphere source term $I'_K(\mu)$ that starts recursion (44). Details of these calculations may be found in Appendix C.2. As in (43) above, the TOA weighting function is determined by relaxing the perturbation ε.

The perturbation analysis described above applies to a single Fourier component (harmonic) of the intensity. The azimuth cosine expansion Eq. (9) applies equally to the weighting functions defined in (43) and (44), namely,

$$\mathscr{K}_{jp}(x, \phi_0 - \phi) = \sum_{m=0}^{2N-1} \mathscr{K}^m_{jp}(x)\cos m(\phi_0 - \phi), \tag{45}$$

where x is the parameter undergoing variation. In this work, a separate convergence test is not applied to the series in Eq. (45); we continue to rely on the convergence criterion applied to the unperturbed intensity field.

3.5. Albedo weighting functions

To derive an albedo weighting function, a relative perturbation is applied to the albedo: $R' = R(1 + \varepsilon)$. This perturbation does not affect layer optical depths and single-scatter albedos so

we can use the original homogeneous solutions and particular integrals in all layers. We then have only to solve for the perturbed integration constants $N_{p\alpha}(R)$ and $P_{p\alpha}(R)$ relevant to this problem. The surface boundary condition will require special consideration for an albedo variation (call this condition BCL6R), but for the other levels BCL1 and BCL2 as described in Section 3.3 will apply. Once again, the determination of the perturbed-field integration constants will emerge from the solution of the linear system $\mathscr{A}\mathscr{X}^* = \mathscr{B}^*$, where the column vector $\mathscr{B}^*(R)$ now depends uniquely on the albedo perturbation. The derivations of BCL6R and the associated vector $\mathscr{B}^*(R)$ are given in Appendix B.

The TOA albedo weighting function is given at the quadrature streams by

$$\mathscr{K}_{jp}(R) = R\frac{\partial I_{jp}}{\partial R} = \lim_{\varepsilon\to 0}\frac{I'_{jp} - I_{jp}}{\varepsilon} \quad \text{for } p = 1 \text{ and } \tau = 0. \tag{46}$$

The post-processed albedo weighting function is easy to establish. Since there is no layer variation, we can use the recursion relation (36) and the source function terms (37) for the original solution, together with a new bottom of the atmosphere source function which reflects the albedo variation. Details can be found in Appendix C.2.

Surface emission plays no part in the perturbation analysis for weighting functions with respect to layer parameters that may vary. However, since the surface emissivity depends on the albedo R, its variation must be included when dealing with albedo weighting functions. This consideration applies only to the fundamental Fourier harmonic $m = 0$. If $R' = R(1 + \varepsilon)$ is the albedo perturbation, then from the definition in Eq. (21), the perturbed emissivity is found to be

$$\kappa'(\mu) = \kappa(\mu) + (\kappa(\mu) - 1)\varepsilon. \tag{47}$$

This is true for all values of μ, not just the quadrature streams. Eq. (47) is required in the determination of the perturbed boundary condition BCL6R in the presence of surface emission.

4. The LIDORT model; two weighting function examples

Before discussing the two examples of LIDORT results in Sections 4.4 and 4.5, we summarize the LIDORT package and remark on two practical aspects, the first regarding atmospheric inputs for more than one scatterer, and the second the issue of weighting function verification.

4.1. Implementation of the LIDORT package

The numerical model LIDORT Version 1.1 is based on the theory of the previous two sections. Intensity and weighting function output are determined for the positive (upwelling) direction at TOA ($\tau = 0$), for arbitrary angular direction (μ, ϕ), and for a plane-parallel medium. The number of terms in the Fourier series required for convergence depends on the azimuth angle and the degree of the discrete ordinate approximation. Double-precision arithmetic is used throughout LIDORT; the code is written in FORTRAN 77. For the numerical tools, we used module ASYMTX for the homogeneous solution eigenproblem (extracted from DISORT), and LAPACK modules [25] for all linear matrix algebra systems. The model contains a standardized error handling procedure in

addition to a number of auxiliary routines for both the reading of input data from files, and the generation of result data to file.

LIDORT has been designed as a generic tool to be used in a wide variety of retrieval applications. It is a pure scattering formalism; the detailed physics required to set up the optical inputs for any given application must be supplied by the user. The "atmospheric preparation" interface for LIDORT is one of the most important aspects, and we discuss this in detail for the two examples below. There are no databases or climatologies of atmospheric and optical properties in the model. The LIDORT package is called as a subroutine within a user-defined environment; the usage is similar to that for DISORT [14].

In order to make the model portable and robust, it is necessary to develop a clearly interfaced and well-documented software package that will help the user to find the right application. The LIDORT User's Guide has a description of the complete package, with detailed notes on the input variables required to run the model, a discussion with examples on the construction of a typical environment for the model and an interface to set up the appropriate geophysical inputs. The User's Guide also contains instructions on installation and execution. A test data set has been prepared for release; this is based closely on the example described in detail in Section 4.5. The LIDORT source code and User's Guide may be downloaded from the SAO web site (http://cfa-www.harvard.edu/lidort/).

4.2. Treatment with several scatterers

In most practical applications, there are often two or more scatterers present (for example in terrestrial atmospheres). Although the theory of Sections 2 and 3 was presented for a single scatterer, it is straightforward to extend the equations to deal with two or more particulates. For an intensity-only calculation, we can define a *combined* single-scatter albedo ω_q and phase function moments β_{lq} for layer q:

$$\omega_q = \sum_d \omega_{qd} \quad \text{and} \quad \beta_{lq} = \sum_d \frac{\beta_{lqd}\omega_{qd}}{\omega_q}, \tag{48}$$

where d is an index for the scatterers and l for the phase function moment. One can then apply the discrete ordinate formalism using the quantities defined in (48); the combination $\omega_q\beta_{lq}$ appears in the Legendre polynomial sums (14). (DISORT [14] also uses this kind of input). For the weighting functions, we suppose that atmospheric parameter x_q is varying in layer q, inducing variational changes u_{qxd} in the individual single-scatter albedos ω_{qd}. Using the above combination, we can define a perturbed form $(\omega_q\beta_{lq})' = \omega_q\beta_{lq}(1 + u_{qlx}\varepsilon)$. The combined variational input u_{qlx} is then given by

$$u_{qlx} = \frac{1}{\omega_q\beta_{lq}} \sum_d \beta_{lqd}\omega_{qd}u_{qxd}. \tag{49}$$

One can then proceed with the perturbation theory as described in Section 3. These considerations do not apply to the optical depth variation. In the examples below, we will illustrate the generation of input quantities ω_{qd} and u_{qxd}.

4.3. Weighting function verification

All weighting function output may be checked against finite-difference equivalents calculated using independent intensity-only calls to the model for externally perturbed atmospheric conditions. To obtain a "finite-difference" weighting function $\mathscr{K}_{\mathrm{FD}}(x_q)$ with respect to atmospheric parameter x_q in layer q, we apply small relative *external* perturbations $\pm\,\varepsilon_{\mathrm{FD}}$ to x_q. The layer input to the model is reconfigured by using $x_q^+ = x_q(1+\varepsilon_{\mathrm{FD}})$ instead of x_q in layer q, and leaving all other inputs unchanged. The perturbation will change the single-scatter albedo in layer q and the optical depth grid for all levels below and including q. The resulting TOA intensity is denoted $I(x_q^+)$. The simulation is repeated with $x_q^- = x_q(1-\varepsilon_{\mathrm{FD}})$ for the perturbed variable, with the result $I(x_q^-)$. The finite difference approximation to the weighting function is

$$\mathscr{K}_{\mathrm{FD}}(x_q) \simeq \frac{I(x_q^+) - I(x_q^-)}{2\varepsilon_{\mathrm{FD}}}. \tag{50}$$

Although the double quadrature scheme is usual, some extra runs were also carried out using the single scheme over the interval $(1, -1)$. For this latter scheme, we have the additional closed-form expressions for the homogeneous and particular solutions developed in the original work by Chandrasekhar; as noted in Appendix D, these require an initial determination of the roots of the characteristic equation. It is also shown in this appendix that closed-form expressions for the perturbed values of these component solutions can be derived. These alternative expressions allow us to make an independent check on weighting function solutions derived using the usual "eigenproblem-and-linear-algebra" approach to the RTE solution. (The characteristic equation was solved using standard eigenvalue modules [27]; this involves considerably less work than solving the complete eigenproblem).

4.4. LIDORT test for a 5-layer medium with two scatterers

The first example described here is for a 5-layer atmosphere (five layers are sufficient to test all eight of the perturbed boundary conditions in Section 3.3). This example will illustrate the generation of variational inputs u_q and v_q controlling weighting function output. This scenario also provides a shakedown test for the model.

First consider a single homogeneous layer with absorption and scattering coefficients α and σ (per unit depth), and altitude thickness z. The single-scatter albedo is $\omega = \sigma/(\alpha+\sigma)$, and the optical depth is $\tau = z(\alpha+\sigma)$. If we perturb the absorption coefficient α by a relative amount ε, then $\alpha' = \alpha(1+\varepsilon)$, and

$$\omega' = \omega(1+u_a\varepsilon), \quad \text{where } u_a = -\alpha/(\alpha+\sigma), \tag{51a}$$

and

$$\tau' = \tau + v_a\varepsilon, \quad \text{where } v_a = \alpha z. \tag{51b}$$

Similarly if the scattering coefficient σ is perturbed by a relative amount ε, so that $\sigma' = \sigma(1+\varepsilon)$, then

$$\omega' = \omega(1+u_s\varepsilon), \quad \text{where } u_s = \alpha/(\alpha+\sigma), \tag{52a}$$

and

$$\tau' = \tau + v_s\varepsilon, \quad \text{where } v_s = \sigma z. \tag{52b}$$

Thus for a single layer specified solely by absorption and scattering coefficients, the parameter variations $\{u_a, v_a\}$ and $\{u_s, v_s\}$ must be input to LIDORT in order to obtain weighting functions with respect to these coefficients.

We now extend these arguments to a 5-layer atmosphere with two particulates. Let the absorption and scattering coefficients be α_{qd} and σ_{qd}, with $q = 1, \ldots, 5$, indexing the layers, and $d = 1, 2$ indexing particulates, along with altitude thickness values z_q. The layer optical thickness values are $\delta_q = e_q z_q$, where the layer extinction is $e_q = \alpha_{q1} + \sigma_{q1} + \alpha_{q2} + \sigma_{q2}$. Single-scatter albedos are $\omega_{qd} = \sigma_{qd}/e_q$. The two particulates have layer phase function moments β_{lq1} and β_{lq2}, where $l = 0, \ldots, 2N - 1$. Phase function moments for this test case can be generated by assuming the Henyey–Greenstein phase envelope (see for example [28]), for which the moments are powers of the asymmetry parameters g_{qd}, that is, $\beta_{lqd} = (g_{qd})^l$. Table 1 summarizes all the optical properties used in this example.

In a given layer q, there are four possibilities for the parameter x_q, namely the absorption coefficient of particulate 1, the scattering coefficient of particulate 1, the absorption coefficient of particulate 2, or the scattering coefficient of particulate 2. (In Eq. (53) below, we keep this ordering). Now let u_{qdx} be the perturbations induced in ω_{qd} by x_q, that is, $\omega'_{qd} = \omega_{qd}(1 + \varepsilon u_{qdx})$. Let v_{qx} be the corresponding changes induced in optical thickness values τ_q. By the reasoning used to derive Eqs. (51) and (52), we have for this scenario:

$$u_{q1x} = \begin{bmatrix} -\alpha_{q1}/e_q \\ 1 - \sigma_{q1}/e_q \\ -\alpha_{q2}/e_q \\ -\sigma_{q2}/e_q \end{bmatrix}, \qquad u_{q2x} = \begin{bmatrix} -\alpha_{q1}/e_q \\ -\sigma_{q1}/e_q \\ -\alpha_{q2}/e_q \\ 1 - \sigma_{q2}/e_q \end{bmatrix} \quad \text{and} \quad v_{qx} = \begin{bmatrix} \alpha_{q1} z_q \\ \sigma_{q1} z_q \\ \alpha_{q2} z_q \\ \sigma_{q2} z_q \end{bmatrix}. \tag{53}$$

Table 1
Setup for 5-layer test of LIDORT

Property/layer	1	2	3	4	5
Absorption coefficient, scatterer 1	0.05	0.17	0.32	0.50	0.35
Absorption coefficient, scatterer 2	0.04	0.18	0.36	0.56	0.37
Scattering coefficient, scatterer 1	0.25	0.25	0.25	0.25	0.25
Scattering coefficient, scatterer 2	0.25	0.26	0.27	0.28	0.29
Layer thickness	0.05	0.05	0.05	0.05	0.05
Cumulative optical depth	0.0295	0.0725	0.1325	0.2120	0.2750
Single scatter albedo, 1	0.42373	0.29070	0.28033	0.15733	0.19841
Single scatter albedo, 2	0.42373	0.30233	0.22500	0.17610	0.23016
Asymmetry parameter, scatterer 1	0.63	0.71	0.69	0.69	0.69
Asymmetry parameter, scatterer 2	0.65	0.70	0.60	0.65	0.65
Thermal emission coefficient b_0	0.2813	0.5684	0.5820	0.5692	−0.7276
Thermal emission coefficient b_1	19.128	9.3951	9.2080	9.3048	15.422

For each layer, the quantities in (53) constitute the required input to the LIDORT model to obtain the desired weighting function output.

The solar zenith angle cosine μ_0 is taken to be 0.75 and the relative azimuth angle 0°. The surface is assumed Lambertian with albedo $R = 0.3$. Thermal emission is omitted from the first set of results. The RTE is solved using eight discrete ordinate streams in the hemisphere. With four possible parameter variations for each of the five layers, there are 20 layer weighting functions in all. LIDORT will generate the TOA intensity and all 20 weighting functions with a single call from a master module. Generation of this set of weighting functions using the external finite-difference approximation (50) would require 40 separate calls to an intensity-only model. In addition to the eight quadrature values, intensity and weighting function output is given at seven user-defined zenith angles, several of which are deliberately chosen close to quadrature values in order to test the accuracy of the post-processing function. With a Fourier azimuth series accuracy criterion of 0.001, seven Fourier terms are required for convergence. All the results in Table 2 are direct-beam normalized (that is, the flux factor $F_\odot$ in Eq. (7) is set to 1).

In this table, DISORT intensity output for the same scenario is presented for comparison; the agreement with the LIDORT values is excellent, with small differences in the last decimal places probably due to the single-precision arithmetic used in DISORT. The last two columns are normalized weighting functions for a variation in layer 3 of the scattering coefficient for particulate 1, calculated first with LIDORT in weighting function mode, and secondly with LIDORT in intensity-only mode calculating finite difference approximations to the weighting functions based on a 2% external perturbation of the scattering coefficient. The results are close, because of the near-linear dependence of the solution on the input optical parameters. Fig. 3 (top) shows the intensity output (stream angles are marked with an asterisk) from Table 2. Note the smooth

Table 2
LIDORT output for relative azimuth 0°

Stream angle in (◦)	LIDORT intensity	DISORT intensity	σ_{31} Weighting function	σ_{31} WF by 2% finite diff.
88.86231[a]	0.105562	0.105592	− 1.623333E-03	− 1.623342E-03
84.16484[a]	0.0661006	0.0661281	− 4.062011E-03	− 4.062021E-03
76.27667[a]	0.0516912	0.0516913	− 3.317248E-03	− 3.317252E-03
65.90300[a]	0.0491804	0.0491682	− 2.687362E-03	− 2.687364E-03
53.72103[a]	0.0490656	0.0490606	− 2.313743E-03	− 2.313744E-03
40.29133[a]	0.0498576	0.0498572	− 2.107697E-03	− 2.107698E-03
26.06016[a]	0.0501983	0.0501983	− 1.989064E-03	− 1.989065E-03
11.43654[a]	0.0504737	0.0504737	− 1.932222E-03	− 1.932223E-03
88.85	0.105363	0.105393	− 1.637481E-03	− 1.637491E-03
80.0	0.0557402	0.0557520	− 3.682994E-03	− 3.683000E-03
76.27	0.0516864	0.0516865	− 3.316667E-03	− 3.316671E-03
45.0	0.0495563	0.0495551	− 2.164834E-03	− 2.164835E-03
30.00	0.0500726	0.0500726	− 2.013753E-03	− 2.013753E-03
11.44	0.0504737	0.0504737	− 1.932232E-03	− 1.932232E-03
0.0	0.0504358	0.0504359	− 1.917111E-03	− 1.917111E-03

[a]Quadrature angles.

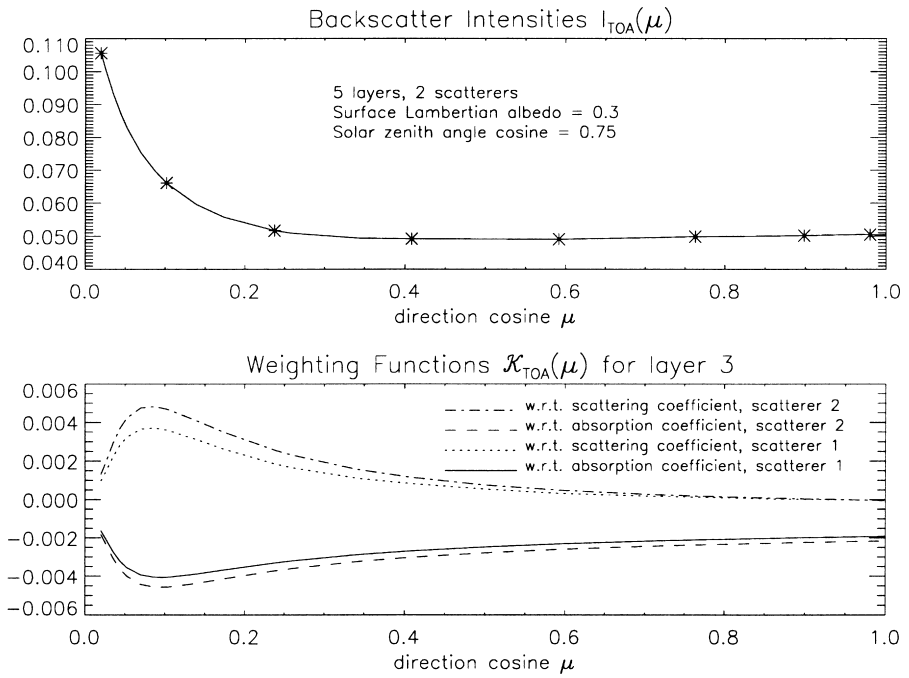

Fig. 3. Intensity and weighting function output for a 5-layer atmosphere, relative azimuth 0°: (top) intensity (quadrature values marked by asterisk); (bottom) weighting functions for layer 3.

interpolation to user-defined zenith angles. Fig. 3 (bottom) are the TOA weighting functions with respect to the absorption and scattering coefficients in layer 3.

Some further runs with this scenario were carried out to test the inclusion of thermal emission source terms. Two thermal expansion coefficients b_{0q} and b_{1q} were computed off-line using the Planck function module in DISORT, for a temperature of 550 K (TOA), and 600, 620, 640, 660, and 680 K at the lower boundaries of the succeeding five layers, and for spectral range of 5000–5100 wavenumbers. The coefficients b_{0q} and b_{1q} are shown in Table 1 in the last two rows (up to a factor of 4π, DISORT takes the same numbers in its computation of the intensity). Using these coefficients enables us to check intensity values against DISORT output. To test the effect of changes in intensity due to thermal emission variations, we assume that any of the optical properties of the atmosphere will induce an identical change in the thermal expansion coefficients. That is, if $\zeta'_q = \zeta_q(1+\varepsilon)$ for property ζ_q, then $b'_{sq} = b_{sq}(1+\varepsilon)$ for each of the thermal expansion coefficients. This means that the perturbation input values defined in Eq. (39d) are $h_{sq} = b_{sq}$ for $s = 0$ and 1. This is obviously not a physical situation, but it serves to check that weighting functions with respect to the Plank function coefficients are being correctly calculated. A similar selection of results for this scenario is shown in Fig. 4.

4.5. Ozone VMR and temperature profile weighting functions in a terrestrial atmosphere

For this example, the atmosphere has height 60 km, with a vertical resolution throughout of 1 km. Molecular (Rayleigh) scattering and aerosol scattering are present in all layers. We take

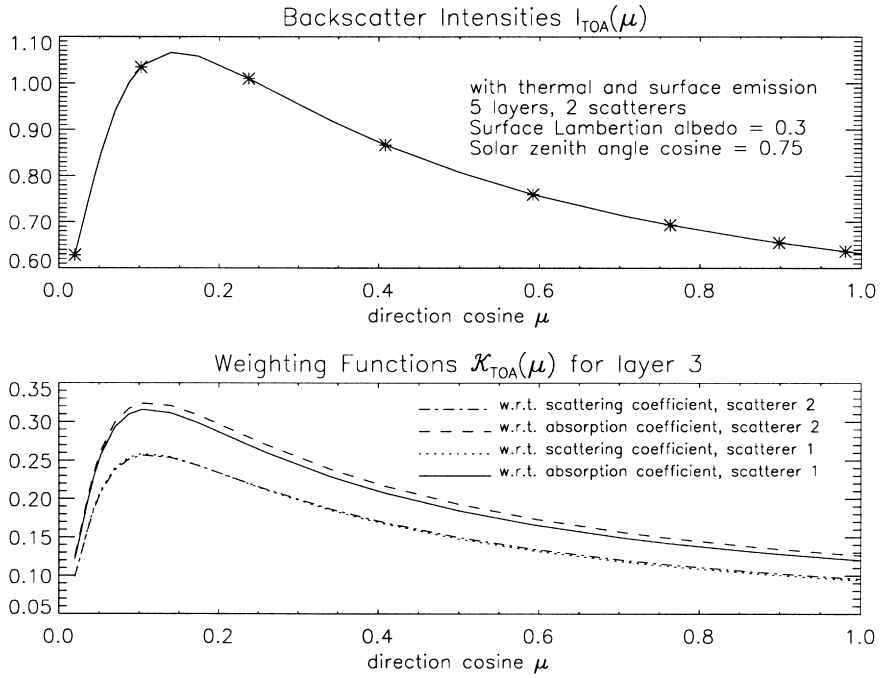

Fig. 4. Intensity and weighting function output for 5-layer atmosphere, relative azimuth 0°, including thermal and surface emission: (top) intensity (quadrature values marked by asterisk); (bottom) weighting functions for layer 3.

O_3 volume mixing ratio (VMR) temperatures and pressures for a "tropical" standard atmosphere [29], interpolated to the mid-points of each layer. The temperature and ozone VMR profiles are shown in Fig. 5.

For the first runs, we take a single wavelength of $\lambda = 324.8863$ nm at one of the peaks of the O_3 Huggins absorption bands; cross section values are obtained from a standard data set [30]. These cross sections ξ are temperature-dependent so they must be evaluated for each layer temperature T_q using the quadratic parameterization [30]:

$$\xi_\lambda(T_q) = \xi_{\lambda 0}\{1 + (T_q - T_0)\xi_{\lambda 1} + (T_q - T_0)^2\xi_{\lambda 2}\}. \tag{54}$$

Here, the first coefficient $\xi_{\lambda 0}$ is the value at reference temperature T_0. If the O_3 VMR in layer q is C_q, and the cross-section is $\xi_\lambda(T_q)$, then the molecular absorption coefficient α_{q1} (in (km^{-1})) is $\alpha_{q1} = C_q\xi_\lambda(T_q)\rho_q$, with the air density ρ_q in $(\mathrm{mol\ cm}^{-2}\ \mathrm{km}^{-1})$ given by $\rho_q = (T_0 P_q/P_0 T_q)\rho_0$, where the zero suffix denotes values at standard temperature and pressure (STP).

The Rayleigh scattering cross-section at STP is given by

$$Q_{\mathrm{Ray}}(T_0) = \frac{32\pi^3(n-1)^2}{3L^2\lambda^4} \times \frac{6 + 3\Delta}{6 - 7\Delta}, \tag{55}$$

where Δ is the depolarization ratio, L is Loschmidt's number, and n is the refractive index of air. Values of Q_{Ray} may be calculated from an empirical formula [31]. Q_{Ray} needs to be multiplied by the layer air density ρ_q to obtain the required scattering coefficient σ_{q1} (km^{-1}). For the aerosol

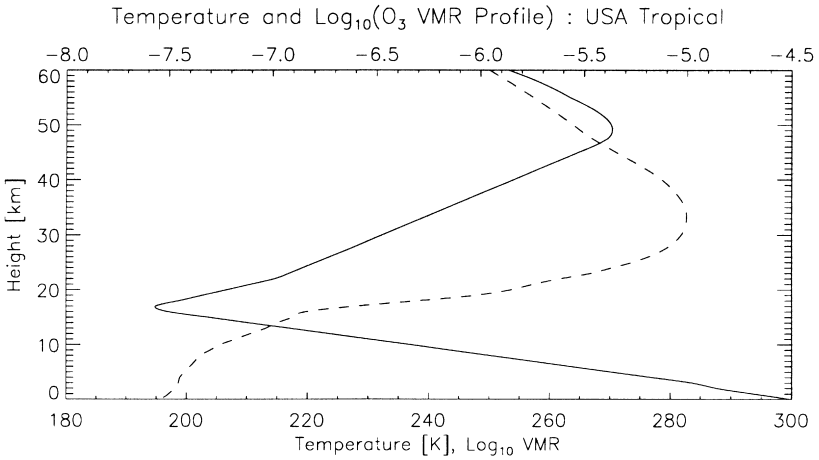

Fig. 5. Temperature and O_3 volume mixing ratio profiles for 0–60 km; "tropical" atmosphere.

loading and optical properties, a LOWTRAN model [32] is selected, with maritime-type boundary layer aerosol and background stratospheric and tropospheric optical properties; values from the database are linearly interpolated to wavelength λ. The resulting optical coefficients (in (km^{-1})) are α_{q2} and σ_{q2}.

The Rayleigh scattering envelope has an $a + b\cos^2\theta$ dependence with respect to scatter angle θ; there are only three terms in the phase function Legendre expansion. The Rayleigh phase function Legendre moments are $\beta_0 = 1$, $\beta_1 = 0$ and $\beta_2 = (1 - \Delta)/(2 + \Delta)$. The depolarization ratio Δ is wavelength-dependent and may be computed from another empirical formula [31]. For the aerosols we assume Henyey–Greenstein phase functions with asymmetry parameters taken from the appropriate choice of LOWTRAN aerosol loading and interpolated to the wavelength of interest. The solar zenith cosine μ_0 is taken to be 0.75, the relative azimuth 60° and the Lambertian surface albedo 0.75. A 10-stream approximation is used in the RTE solution, with accuracy criterion 0.001. All output is normalized to the incident intensity of the direct beam. There is no thermal or surface emission.

We are interested in weighting functions with respect to the O_3 VMR profile distribution C_q. Writing $C'_q = C_q(1 + \varepsilon)$ for the perturbation, we find that

$$u_{q1}(C_q) = u_{q2}(C_q) = -\alpha_{q1}/e_q, \tag{56a}$$

$$v_{q1}(C_q) = \alpha_{q1} z_q. \tag{56b}$$

Here, α_{q1} is the O_3 absorption coefficient and e_q and z_q the total extinction and height thickness for layer q.

For temperature weighting functions, the functional dependence of the optical properties on temperature is more complex. If the relative variation in temperature T_q in layer q is ε, so that $T'_q = T_q(1 + \varepsilon)$, then it follows that $\rho'_q = \rho_q(1 - \varepsilon)$ for the air density, and from Eq. (54) the variation in O_3 cross-section is

$$\xi'_\lambda(T_q) \equiv \xi_q + \varepsilon\eta_q = \xi_\lambda(T_q) + \varepsilon T_q \xi_{\lambda 0}\{\xi_{\lambda 1} + 2(T_q - T_0)\xi_{\lambda 2}\}. \tag{57}$$

Since $Q_{\mathrm{Ray}}(T_q) = \rho_q Q_{\mathrm{Ray}}(T_0)$, and the STP value $Q_{Ray}(T_0)$ has no dependence on T_q, then the variations for the absorption and scattering coefficients are

$$\alpha'_{q1} = \alpha_{q1}[1 - \varepsilon(1 - \eta_q/\xi_q)], \tag{58a}$$

$$\sigma'_{q1} = \sigma_{q1}(1 - \varepsilon). \tag{58b}$$

These in turn lead to the following variational inputs for the layer single-scatter albedos and optical depth required by LIDORT:

$$u_{q1}(T_q) = -(1 + \psi_q/e_q), \quad u_{q2}(T_q) = -\psi_q/e_q \quad \text{and} \quad v_q(T_q) = z_q\psi_q, \tag{59}$$

where

$$\psi_q = \alpha_{q1}(\eta_q/\xi_q - 1) - \sigma_{q1}. \tag{60}$$

Note in particular that the aerosol single-scatter albedo has the non-zero variation $u_{q2}(T_q)$, even though the aerosol coefficients themselves are unaffected by the perturbations.

Fig. 6 (top) shows the intensity output for this scenario at $\lambda = 324.8863$ nm. Quadrature values are marked by an asterisk to illustrate the smoothness of the post-processing function for user-defined zenith angles. Fig. 6 (bottom) shows results for a line-of-sight zenith angle of 30° for the O_3 VMR and temperature weighting functions plotted against altitude; values are normalized

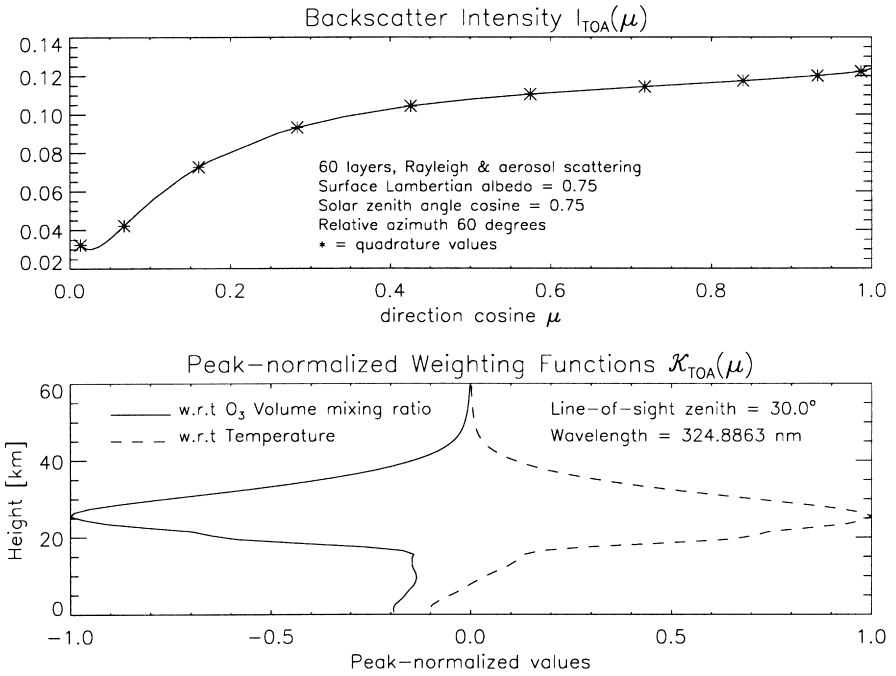

Fig. 6. LIDORT results for a 60-layer atmosphere for wavelength 324,8863 nm, albedo 0.75, relative azimuth 60°, $\mu_0 = 0.75$; (top) sun-normalized TOA intensity at various zenith angles (quadrature streams marked by an asterisk); (bottom) Peak-normalized weighting functions for O_3 VMR and temperature profiles, at zenith angle 30°.

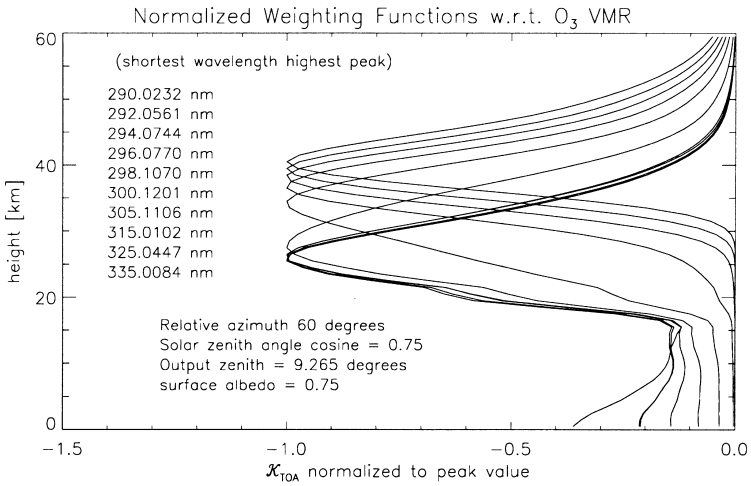

Fig. 7. LIDORT weighting functions for O_3 VMR for a 60-layer atmosphere for a number of wavelengths in the UV, for zenith angle 9.265°.

to the peak values in each case. The sensitivity of both functions around the peak O_3 concentration level is evident.

In Fig. 7, O_3 VMR weighting functions are presented for a number of wavelengths in the UV from 290 to 335 nm as indicated (these wavelengths are used as found in the data set [30]; their use obviates the need for interpolation of cross-section values). Below 300 nm, peak values occur at heights that increase with lower wavelengths. It is this well-known differential scattering height behaviour that underpins the BUV technique for O_3 profile retrieval [5,6]. Note also the increasing tropospheric sensitivity for the longer wavelengths.

Finally a comparison is made with results from the GOMETRAN [17] model computed at $\lambda = 324.8863$ nm for the same atmosphere. GOMETRAN input profiles are given at 61 levels from 0 to 60 km. O_3 cross-sections are given by Eq. (54) for temperatures at the layer boundaries. Fig. 8 gives the comparison for O_3 VMR weighting functions at stream angle 9.265° (one of the quadrature values). The agreement between these two independently calculated results is excellent, with differences of 1% or less at virtually all levels away from the shoulder near 17 km. Here the O_3 concentration gradient changes sharply, and the 1 km height resolution of the models is not fine enough to ensure "layer-versus-level" interpolation errors are kept to a minimum.

5. Summary and future developments

In this paper we have developed an extension of the discrete ordinate solution of the radiative transfer equation in a plane parallel, multiply scattering, anisotropic, multilayer atmosphere with beam and thermal emission sources. The extension is essentially an internal perturbation analysis of the discrete ordinate solution, and along with standard intensity output, it allows for the simultaneous calculation of analytically-accurate weighting function fields with respect to a wide

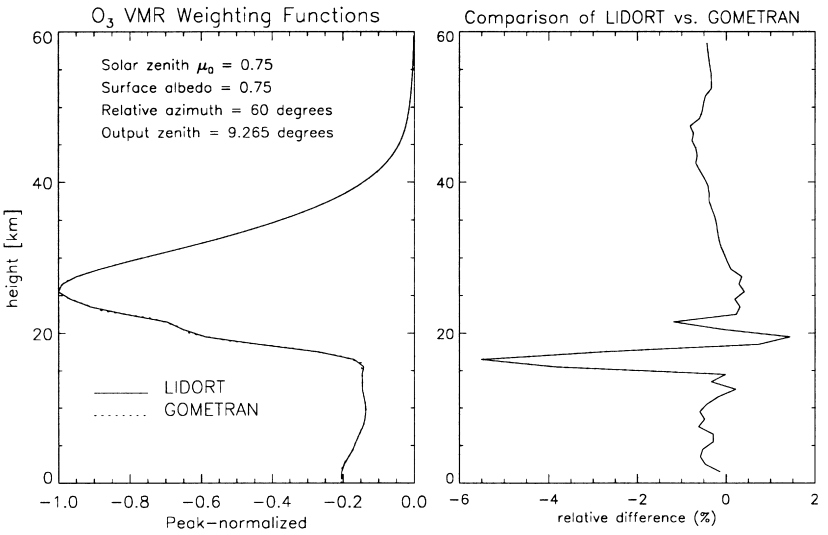

Fig. 8. LIDORT and GOMETRAN weighting functions for O_3 VMR for a 60-layer (61-level) atmosphere for wavelength 324.8863 nm and for zenith angle 9.265°.

variety of atmospheric parameters. This extension avoids the time-consuming procedure of using external perturbation calculations to approximate the weighting functions. A numerical model (LIDORT) has been constructed and tested for two scenarios, one of which is a representative terrestrial atmosphere with ozone absorption and molecular and aerosol scattering. The model is generic in character, requiring as the main input the single-scatter albedos and grid optical depths, plus variations induced on these inputs by the set of parameters for which the weighting functions are to be computed. These application-specific inputs are defined by the user, and they depend on the physics of the atmosphere under consideration.

The model described here has recently been extended to cover a much wider range of scenarios; intensity and weighting function output is now available for upwelling and downwelling directions, at arbitrary optical depth and stream angle. A "pseudo-spherical" treatment of the direct beam attenuation has also been implemented in the new version of LIDORT. This gives the model the power to accommodate solar zenith angles up to 90° (c.f. [33]). There is also the option to treat sharply peaked phase functions using the delta-M scaling approximation [34]. LIDORT Version 2.1 is now available from the SAO website; the new version will be described in a companion paper to the present work (R. Spurr, in preparation).

The implementation of a vectorized radiative transfer code to give a full Stokes-vector treatment of the perturbed discrete ordinate solution is also under consideration. The intensity-only problem has been analyzed, and there now exists a robust vectorized DISORT [35,36].

Acknowledgements

This work was supported in part by a contract from the Deutsches Forschunszentrum für Luft und Raumfahrt, contract number 332/60570480 (SCIAMACHY Data Processor Development),

and in part with internal funding from the Smithsonian Astrophysical Observatory. Special thanks are due to Knut Stamnes for helpful suggestions regarding the manuscript.

Appendix A. Perturbation analysis for the discrete ordinate component solutions

In this appendix the perturbation factors defined in Eqs. (40a)–(40d) are established. We consider a single layer and Fourier component, omitting the respective indices for the sake of clarity.

A.1. Homogeneous solution

Consider first the eigenvalue problem Eq. (22) and associated definitions in Eq. (23). The perturbation rule $\omega' = \omega(1 + u\varepsilon)$ applies to the single-scatter albedo, and since the eigenmatrix and its eigensolutions are proportional to ω, then they will also perturb in a similar fashion. Define the first-order perturbation for the eigenmatrix Γ in Eq. (22) as follows:

$$\Gamma'_{ij} = \Gamma_{ij} + u\varepsilon\xi_{ij} = \sum_{l=1}^{N} (\zeta'_{il} - \eta'_{il})(\zeta'_{lj} + \eta'_{lj}). \tag{A.1}$$

Since the $D^{\pm}_{ij}$ in Eq. (23) depend linearly on ω, their first-order perturbed values are given by $D^{\pm}_{ij}{}' = D^{\pm}_{ij}(1 + u\varepsilon)$. From the definitions of matrices ζ_{ij} and η_{ij}, we obtain

$$\zeta'_{ij} = \zeta_{ij} + u\varepsilon a_j D^{+}_{ij}\mu_i^{-1} \quad \text{and} \quad \eta'_{ij} = \eta_{ij} + u\varepsilon a_j D^{-}_{ij}\mu_i^{-1}. \tag{A.2}$$

Substituting Eqs. (A.2) in Eq. (A.1), we get the following determination of ξ_{ij}:

$$\xi_{ij} = \sum_{l=1}^{N} \left\{ \frac{a_l C^{-}_{il}}{\mu_i}(\zeta_{lj} + \eta_{lj}) + (\zeta_{il} - \eta_{il})\frac{a_j C^{+}_{lj}}{\mu_l} \right\}, \tag{A.3}$$

where $C^{\pm}_{ij} = D^{+}_{ij} \pm D^{-}_{ij}$.

Next, we have the perturbed version of the eigenproblem of Eq. (22):

$$\sum_{j=1}^{N} \Gamma'_{ij}\varsigma'_{j\alpha} = k'^{\,2}_{\alpha}\varsigma'_{i\alpha} \quad \text{for } i = 1, \ldots, N,\ \alpha = 1, \ldots, N. \tag{A.4}$$

The eigenvalues perturb as $k'_\alpha = k_\alpha + u\varepsilon f_\alpha$. For the eigenvector perturbation, we define $\varsigma'_{j\alpha} = \varsigma_{j\alpha} + u\varepsilon\Upsilon_{j\alpha}$. In order to find scalar f_α and vector $\Upsilon_{j\alpha}$ for each α, we use the result of Eq. (A.3) in (A.4) and remove the zero-order term using the original eigenvalue (22). This gives the following N equations satisfied by the first-order term:

$$\sum_{j=1}^{N} (\Gamma_{ij}\Upsilon_{j\alpha} + \xi_{ij}\varsigma_{j\alpha}) = k_\alpha^2\Upsilon_{i\alpha} + 2k_\alpha f_\alpha\varsigma_{i\alpha} \quad \text{for } i = 1, \ldots, N. \tag{A.5}$$

Since there are $N + 1$ unknowns $\{f_\alpha, \Upsilon_{i\alpha}\}$ for each α, an additional condition is required in order to find the solution. This comes from the normalization condition (26). If the perturbed vector also has unit normalization, then $\|\varsigma'^{\,2}_{\alpha}\| = 1$; from the definition of this vector, we get the following for the

first-order term:

$$\sum_{j=1}^{N} \Upsilon_{j\alpha}\varsigma_{j\alpha} = 0. \tag{A.6}$$

Eqs. (A.5) and (A.6) are now combined in a linear system of order $N+1$. Define vectors Q_α and B_α and matrix A_α as follows:

$$Q_\alpha = \begin{bmatrix} f_\alpha \\ \Upsilon_{1\alpha} \\ \Upsilon_{2\alpha} \\ \vdots \\ \Upsilon_{N\alpha} \end{bmatrix}, \quad B_\alpha = \begin{bmatrix} \sum_j \xi_{1j}\varsigma_{j\alpha} \\ \sum_j \xi_{2j}\varsigma_{j\alpha} \\ \vdots \\ \sum_j \xi_{Nj}\varsigma_{j\alpha} \\ 0 \end{bmatrix}, \quad A_\alpha = \begin{bmatrix} 2k_\alpha\varsigma_{1\alpha} & k_\alpha^2 - \Gamma_{11} & -\Gamma_{12} & \cdots & -\Gamma_{1N} \\ 2k_\alpha\varsigma_{2\alpha} & -\Gamma_{21} & k_\alpha^2 - \Gamma_{22} & \cdots & -\Gamma_{2N} \\ \vdots & \vdots & \vdots & \ddots & \vdots \\ 2k_\alpha\varsigma_{N\alpha} & -\Gamma_{N1} & -\Gamma_{N2} & \cdots & k_\alpha^2 - \Gamma_{NN} \\ 0 & \varsigma_{1\alpha} & \varsigma_{2\alpha} & \cdots & \varsigma_{N\alpha} \end{bmatrix}. \tag{A.7}$$

Then for each α, the linear algebra system $A_\alpha Q_\alpha = B_\alpha$ is solved to obtain the vector Q_α of desired perturbation values. (In the model, LAPACK linear algebra routines DGETRF and DGETRS were used for the numerical solution of this system). This completes the perturbation analysis of the eigenproblem.

The perturbed version of the auxiliary relation (24) is

$$k'_\alpha \vartheta'_{i\alpha} = \sum_{j=1}^{N} (\zeta'_{ij} + \eta'_{ij})\varsigma'_{j\alpha}. \tag{A.8}$$

We now make the definition $\vartheta'_{i\alpha} = \vartheta_{i\alpha} + u\varepsilon\chi_{i\alpha}$ for the perturbation of the difference vector ϑ. Using the results obtained so far for f_α and $\Upsilon_{j\alpha}$, together with (A.2), and concentrating on the first-order term in (A.8), we find after some manipulation that vectors χ_α have components

$$\chi_{i\alpha} = \frac{1}{k_\alpha}\left\{ \sum_{j=1}^{N} \left[\frac{a_j C_{ij}^+}{\mu_i}\varsigma_{j\alpha} + (\zeta_{ij} + \eta_{ij})\Upsilon_{j\alpha} \right] - f_\alpha \vartheta_{i\alpha} \right\} \quad \text{for } i = 1, \ldots, N. \tag{A.9}$$

Having completed the perturbation analysis for the sum and difference vectors ς_α and ϑ_α, perturbation factors $Y_{i\alpha}^{\pm}$ for the actual homogeneous solution vectors follow from the relations

$$\chi_{i\alpha} = Y_{i\alpha}^{+} - Y_{i\alpha}^{-} \quad \text{and} \quad \Upsilon_{i\alpha} = Y_{i\alpha}^{+} + Y_{i\alpha}^{-}. \tag{A.10}$$

Application of the symmetry relations $Y_{-i\alpha}^{+} = Y_{i\alpha}^{-}$ and $Y_{-i\alpha}^{-} = Y_{i\alpha}^{+}$ (cf. (25)) completes the perturbation analysis of the homogeneous solution.

A.2. Particular solutions

The particular solution for the beam source is determined from Eq. (27). The perturbed version of this equation is

$$\sum_{j=-N}^{N} A_{ij}^{\prime(\text{beam})} W'_j = B_i^{\prime(\text{beam})}. \tag{A.11}$$

The definitions of $A^{(\text{beam})}$ and $B^{(\text{beam})}$ in (28) indicate that they are linearly dependent on the single-scatter albedo ω. Hence the first-order perturbed values are

$$A'^{(\text{beam})}_{ij} = A^{(\text{beam})}_{ij} - u\varepsilon a_j D_{ij} \quad \text{and} \quad B'^{(\text{beam})}_{i} = B^{(\text{beam})}_{i}(1 + u\varepsilon). \tag{A.12}$$

Since $W'_i = W_i + u\varepsilon Z_i$ for the perturbed solution, then application of (A.12) in (A.11) yields

$$\sum_j A^{(\text{beam})}_{ij} Z_j = B^{(\text{beam})}_i - \sum_j a_j D_{ij} W_j. \tag{A.13}$$

Since the LU-decomposition of the matrix $A^{(\text{beam})}$ has been found already in the course of determining the original beam solution, the solution for Z follows immediately by back-substitution using the right-hand side of (A.13).

The situation for the thermal emission source term is similar. The recurrence relations in (29) for the expansion coefficients $T_{j,s}$ may be written in the perturbed form

$$\sum_j A'^{(\text{thermal})}_{ij} T'_{j,s} = \begin{cases} (1-\omega')b'_s e_i & \text{for } s = S, \\ (1-\omega')b'_s e_i + (s+1)\mu_i T'_{i,s+1} & \text{for } s < S. \end{cases} \tag{A.14}$$

The definition of the matrix $A^{(\text{thermal})}$ implies that $A'^{(\text{thermal})}_{ij} = A^{(\text{thermal})}_{ij} - u\varepsilon a_j D_{ij}$. From the definitions $b'_s = b_s + \varepsilon h_s$, $T'_{j,s} = T_{j,s} + \varepsilon V_{j,s}$ and using (A.14), the following recurrence relations for the first-order perturbation factors $V_{j,s}$ are found:

$$\sum_j A^{(\text{thermal})}_{ij} V_{j,s} = \begin{cases} [(1-\omega)h_s - ub_s\omega]e_i + u\sum_j a_j D_{ij} T_{j,s} & \text{for } s = S, \\ [(1-\omega)h_s - ub_s\omega]e_i + u\sum_j a_j D_{ij} T_{j,s} + (s+1)\mu_i V_{i,s+1} & \text{for } s < S. \end{cases} \tag{A.15}$$

The LU-decomposition of the matrix $A^{(\text{thermal})}$ is known already from the original determination of vector T, and thus the solution for the coefficients V follows by back-substitution in (A.15). This completes the perturbation analysis of the RTE particular solutions.

Appendix B. Boundary conditions for the perturbed field

We will establish here the eight boundary conditions summarized in Section 3.3 and indicated in Fig. 2 for the atmospheric layer weighting functions. Only the beam particular integral terms will be included in the full boundary condition equations that follow; however, we indicate the additional contributions needed for atmospheric thermal emission. The calculation of TOA weighting functions is also described. Finally, we determine the special boundary condition BCL6R required for the albedo perturbation problem.

B.1. BCL1 (Cases 1 and 3)

At the top of the atmosphere, the perturbed downwelling intensity is zero, that is, $I'_{-jp} = 0$ for $\tau = 0$, $p = 1$ and $j = 1, \ldots, N$. There is no variation in this layer, so $k'_{p\alpha} = k_{p\alpha}$, $X'_{jp\alpha} = X_{jp\alpha}$, and $W'_{jp} = W_{jp}$ for the homogeneous and particular solutions; we have only to consider perturbations

of the integration constants as defined in (41a) and (41b). The first-order perturbed intensity for this layer is then

$$I'_{-jp} = I_{-jp} + \varepsilon \sum_{\alpha=1}^{N} \{N_{p\alpha} e^{-k_{p\alpha}(\tau-\tau_{p-1})} X^{+}_{-jp\alpha} + P_{p\alpha} e^{-k_{p\alpha}(\tau_p-\tau)} X^{-}_{-jp\alpha}\}. \tag{B.1}$$

Since $I_{-jp}(\tau_0) = 0$ for the original (unperturbed) boundary condition BC1, BCL1 for $p = 1$ may be written as

$$\sum_{\alpha=1}^{N} [N_{p\alpha} X^{+}_{-jp\alpha} + P_{p\alpha}\Theta_{p\alpha} X^{-}_{-jp\alpha}] = U_j^{(1)} \quad \text{(BCL1)}, \tag{B.2}$$

where $U_j^{(1)} = 0$. As before, the transmittance factor is given by $\Theta_{p\alpha} = \exp(-k_{p\alpha}\Delta_p)$, with $\Delta_p = \tau_p - \tau_{p-1}$ the layer optical thickness. Note the similarity to BC1 in (34a).

B.2. BCL2 (Cases 1 and 3)

This applies to all layers p such that $1 < p < q$ (q is the varying layer). As with BCL1, the RTE solutions remain unperturbed in these layers, and Eq. (B.1) applies for both positive and negative stream angles. At the boundary between layer $r = p - 1$ and layer p, the optical depth is τ_r and continuity across this boundary yields BCL2 for $j = \pm 1, \ldots, \pm N$:

$$\sum_{\alpha=1}^{N} \{N_{r\alpha}\Theta_{r\alpha} X^{+}_{jr\alpha} + P_{r\alpha} X^{-}_{jr\alpha}\} - \sum_{\alpha=1}^{N} \{N_{p\alpha} X^{+}_{jp\alpha} + P_{p\alpha}\Theta_{p\alpha} X^{-}_{jp\alpha}\} = U_{jp}^{(2)} \quad \text{(BCL2)}, \tag{B.3}$$

where $U_{jp}^{(2)} = 0$. Again the similarity to BC2 in Eq. (34b) is clear.

B.3. BCL3 (Cases 1 and 3)

This is the upper boundary of the layer q that is varying ($q > 1$ for this condition). If $p = q - 1$, the boundary condition is $I'_{jp} = I'_{jq}$ at $\tau = \tau_p$. In layer p, there is no variation of the RTE solutions, so we can use an expression like (B.1) for the perturbed field. For layer q, we must use the expression in Eq. (42a) together with the perturbed RTE solution variables $k'_{q\alpha}$, $X'_{jq\alpha}$ and W'_{jq}, with perturbation factors $f_{q\alpha}$, $Y_{jq\alpha}$ and Z_{jq} as derived from Section 3.2 and Appendix A. Since $\tau'_q = \tau_q + v_q\varepsilon$ and $\tau'_p = \tau_p$, we can expand the exponential factors in (42a) to first order in ε:

$$e^{-k'_{q\alpha}\tau'_p} = e^{-k_{q\alpha}\tau_p}(1 - \varepsilon u_q f_{q\alpha}\tau_p) \tag{B.4a}$$

and

$$e^{-k'_{q\alpha}\tau'_q} = e^{-k_{q\alpha}\tau_q}(1 - \varepsilon u_q f_{q\alpha}\tau_q - \varepsilon v_q k_{q\alpha}). \tag{B.4b}$$

In the perturbed boundary condition, the zero-order term is eliminated by using the original unperturbed boundary condition BC2. Collecting all terms of order ε, and using (B.4a) and (B.4b), the condition BCL3 for $j = \pm 1, \ldots, \pm N$ is written

$$\sum_{\alpha=1}^{N} \{N_{p\alpha}\Theta_{p\alpha} X^{+}_{jp\alpha} + P_{p\alpha} X^{-}_{jp\alpha}\} - \sum_{\alpha=1}^{N} \{N_{q\alpha} X^{+}_{jq\alpha} + P_{q\alpha}\Theta_{q\alpha} X^{-}_{jq\alpha}\} = U_{jq}^{(3)} \quad \text{(BCL3)}. \tag{B.5}$$

Here, we have the auxiliary vector

$$U_{jq}^{(3)} = u_q Z_{jq} \mathrm{e}^{-\tau_p/\mu_0} + \sum_{\alpha=1}^{N} \{L_{q\alpha} u_q Y_{jq\alpha}^{+} + M_{q\alpha}\Theta_{q\alpha}(u_q Y_{jq\alpha}^{-} - \varpi_{q\alpha} X_{jq\alpha}^{-})\}, \tag{B.6}$$

where

$$\varpi_{q\alpha} = u_q f_{q\alpha}\Delta_q + v_q k_{q\alpha}. \tag{B.7}$$

B.4. BCL4 (Cases 1 and 2)

This is the lower boundary of the layer q that is varying ($q < K$ for this condition). If now $p = q + 1$ the boundary condition is $I'_{jq} = I'_{jp}$ at $\tau = \tau'_q$. In layer p, there is no variation of the RTE solutions so an expression of type (42c) applies for the perturbed field, whereas for layer q, (42a) is appropriate. In addition to the expressions (B.4a) and (B.4b) there is the following first-order expansion for the beam solution exponential term

$$\mathrm{e}^{-\tau'_q/\mu_0} = \mathrm{e}^{-\tau_q/\mu_0}\left[1 - \varepsilon\frac{v_q}{\mu_0}\right]. \tag{B.8}$$

The zero-order term is again removed by using the original BC2 boundary condition, and with the help of (B.4a), (B.4b) and (B.8), BCL4 for $j = \pm 1, \ldots, \pm N$ may be written as

$$\sum_{\alpha=1}^{N} \{N_{q\alpha}\Theta_{q\alpha} X_{jq\alpha}^{+} + P_{q\alpha} X_{jq\alpha}^{-}\} - \sum_{\alpha=1}^{N} \{N_{p\alpha} X_{jp\alpha}^{+} + P_{p\alpha}\Theta_{p\alpha} X_{jp\alpha}^{-}\} = U_{jq}^{(4)} \quad \text{(BCL4)}, \tag{B.9}$$

where

$$U_{jq}^{(4)} = \left(-E_{jq} - \frac{v_q W_{jp}}{\mu_0}\right)\mathrm{e}^{-\tau_q/\mu_0} - \sum_{\alpha=1}^{N} \{L_{q\alpha}\Theta_{q\alpha}(u_q Y_{jq\alpha}^{+} - \varpi_{q\alpha} X_{jq\alpha}^{+}) + M_{q\alpha} u_q Y_{jq\alpha}\}. \tag{B.10}$$

$\varpi_{q\alpha}$ is defined in (B.7) and

$$E_{jq} = u_q Z_{jq} - \frac{v_q W_{jq}}{\mu_0}. \tag{B.11}$$

B.5. BCL5 (Cases 1 and 2)

In this case, the boundary lies between layers p and $r = p - 1$, where $r > q$ and $q < K$. The only perturbation is with the optical depth boundary value $\tau'_r = \tau_r + v_q\varepsilon$, and perturbed fields of type (42c) apply to both layers. Again using the original BC2 condition to remove the zero-order term, the first-order term is written as BCL5 for $j = \pm 1, \ldots, \pm N$:

$$\sum_{\alpha=1}^{N} \{N_{r\alpha}\Theta_{r\alpha} X_{jr\alpha}^{+} + P_{r\alpha} X_{jr\alpha}^{-}\} - \sum_{\alpha=1}^{N} \{N_{p\alpha} X_{jp\alpha}^{+} + P_{p\alpha}\Theta_{p\alpha} X_{jp\alpha}^{-}\} = U_{jp}^{(5)} \quad \text{(BCL5)}, \tag{B.12}$$

where

$$U_{jp}^{(5)} = \frac{v_q}{\mu_0} e^{-\tau_r/\mu_0}(W_{jr} - W_{jp}). \tag{B.13}$$

B.6. BCL6 (*Cases 1 and 2*)

Here $p = K$, the final layer, and the boundary is the bottom surface, with the diffuse radiation satisfying the reflection condition. The optical depth variation is $\tau'_p = \tau_p + v_q\varepsilon$; the single-scatter albedo has no variation. We require the diffusely reflected intensities (these appeared in BC3 in Section 2). We will require also the quantities $\Phi_{j\alpha}^{\pm}$ in (35a) and Ψ_j in (35b). The reflection condition includes the surface source term I_j^* defined in (33). Leaving aside the surface emission contribution, perturbations of I_j^* are generated by the change in optical depth at the lower boundary. Thus

$$I'_j{}^* = I_j^*\left(1 - \frac{v_q\varepsilon}{\mu_0}\right). \tag{B.14}$$

to first order. Bringing together the relevant terms, and using BC3 to eliminate the zero-order terms, the boundary condition BCL6 for $j = 1, \ldots, N$ is

$$\sum_{\alpha=1}^{N} [N_{p\alpha}\Theta_{p\alpha}\Phi_{j\alpha}^{+} + P_{p\alpha}\Phi_{j\alpha}^{-}] = U_j^{(6)} \quad \text{(BCL6)}, \tag{B.15}$$

where

$$U_j^{(6)} = \frac{v_q}{\mu_0}[\Psi_j e^{-\tau_p/\mu_0} - I_j^*]. \tag{B.16}$$

Once again, we note the similarity in the left-hand side of BCL6 to that in BC3 (34c).

B.7. BCL3M (*Case 2 only*)

This is really a combination of BCL1 and BCL3, wherein the upper boundary of the layer that is varying happens to be the top of the atmosphere. Since $q = 1$ for this case, the boundary condition is $I'_{-jq} = 0$ at $\tau_{q-1} = 0$. We take the BCL3 result above, ignore the term in the left-hand side involving layer $p = q - 1$ (which does not exist at TOA), and set $\tau_p = 0$ in (B.6). The result is BCL3M for $j = 1, \ldots, N$:

$$\sum_{\alpha=1}^{N} \{N_{q\alpha}X_{-jq\alpha}^{+} + P_{q\alpha}\Theta_{q\alpha}X_{-jq\alpha}^{-}\} = U_j^{(3M)} \quad \text{(BCL3M)}, \tag{B.17}$$

where

$$U_j^{(3M)} = -u_q Z_{-jq} - \sum_{\alpha=1}^{N} \{L_{q\alpha}u_q Y_{-jq\alpha}^{+} + M_{q\alpha}\Theta_{q\alpha}(u_q Y_{-jq\alpha}^{-} - \varpi_{q\alpha}X_{-jq\alpha}^{-})\}. \tag{B.18}$$

B.8. BCL4M (*Case 3 only*)

This is a combination of the conditions BCL4 and BCL6 with $q = K$. At the bottom boundary, the optical depth variation is $\tau'_q = \tau_q + v_q\varepsilon$. All of the exponential variations in (B.4a), (B.4b) and (B.8) are now required, since both the homogeneous solutions and the particular integral are perturbed in this layer. Both the original and the perturbed diffuse intensities must now satisfy the reflection condition. Thus in addition to the quantities Φ and Ψ in (35a) and (35b) defined for unperturbed solutions $X_{jq\alpha}$ and W_{jq}, we must define similar quantities for the perturbation terms $Y_{jq\alpha}$ and E_{jq} (the latter is defined in (B.11)). Let

$$\Xi^{\pm}_{j\alpha} = Y^{\pm}_{jq\alpha} - (1 + \delta_{m0})R \sum_{i=1}^{N} a_i\mu_i\rho^*_m(\mu_j, -\mu_i)Y^{\pm}_{-iq\alpha} \tag{B.19}$$

and

$$F_j = E_{jq} - (1 + \delta_{m0})R \sum_{i=1}^{N} a_i\mu_i\rho^*_m(\mu_j, -\mu_i)E_{-iq}. \tag{B.20}$$

Combining all the variations for this case, and including the variation of the direct beam from (B.14), BCL4M for $j = 1, \ldots, N$ is

$$\sum_{\alpha=1}^{N} \{N_{q\alpha}\Theta_{q\alpha}\Phi^{+}_{j\alpha} + P_{q\alpha}\Phi^{-}_{j\alpha}\} = U^{(4M)}_j \quad \text{(BCL4M)}, \tag{B.21}$$

where

$$U^{(4M)}_j = -F_j e^{-\tau_q/\mu_0} - \frac{v_q}{\mu_0} I^*_j - \sum_{\alpha=1}^{N} \{L_{q\alpha}\Theta_{q\alpha}(u_q\Xi^{+}_{j\alpha} - \varpi_{q\alpha}\Phi^{+}_{j\alpha}) + M_{q\alpha}u_q\Xi^{-}_{j\alpha}\}. \tag{B.22}$$

An examination of the left-hand sides of all these eight conditions shows that the boundary value problem for $N_{p\alpha}$ and $P_{p\alpha}$ has the same form as that for the original integration constants $L_{p\alpha}$ and $M_{p\alpha}$. Thus, as indicated in Section 3.3, the solution has the form $\mathscr{X}^* = \mathscr{A}^{-1}\mathscr{B}^*$, where the matrix $\mathscr{A}$ is the same as that used in the unperturbed boundary value problem, and the column vector $\mathscr{B}^*$ is constructed from the appropriate combination of vectors $U^{(1)}$, $U^{(2)}_q$, $U^{(3)}_q$, $U^{(4)}_q$, $U^{(5)}_q$, $U^{(6)}$, $U^{(3M)}$ and $U^{(4M)}$, the exact choice depending on the layer q containing the variation in parameter x_q.

B.9. *TOA weighting function output*

Assuming now that the perturbed boundary problem has been solved for $N_{p\alpha}$ and $P_{p\alpha}$, we use definition (43) to calculate the weighting functions at positive computational angles at the top of the atmosphere. We distinguish between Cases 1 and 3 ($q > 1$), where the variation is with respect to parameter x_q in a layer below the first one, and Case 2 ($q = 1$), where the variation is actually in the top layer. For Cases 1 and 3:

$$\mathscr{K}_{jp}(x_q) = \lim_{\varepsilon\to 0} \frac{I'_{jp} - I_{jp}}{\varepsilon} = \sum_{\alpha=1}^{N} \{N_{p\alpha}X^{+}_{jp\alpha} + P_{p\alpha}\Theta_{p\alpha}X^{-}_{jp\alpha}\}, \tag{B.23}$$

where $j = 1, \ldots, N$ and $p = 1$. For Case 2 ($q = 1$):

$$\mathscr{K}_{jq}(x_q) = \sum_{\alpha=1}^{N} \{N_{q\alpha} X^{+}_{jq\alpha} + P_{q\alpha}\Theta_{q\alpha} X^{-}_{jq\alpha}\} + Q^{(3M)}_{j}, \tag{B.24}$$

where

$$Q^{(3M)}_{j} = u_q Z_{jq} + \sum_{\alpha=1}^{N} \{L_{q\alpha} u_q Y^{+}_{jq\alpha} + M_{q\alpha}\Theta_{q\alpha}(u_q Y^{-}_{jq\alpha} - \varpi_{q\alpha} X^{-}_{jq\alpha})\}. \tag{B.25}$$

B.10. Inclusion of atmospheric thermal emission terms in the perturbed boundary conditions

The coefficients $T_{jq,s}$ in the thermal emission particular integral (derived by solving (29)) have first-order perturbations V_{jqs} defined in (40d) only for the layer q that is varying. The solution for $V_{jq,s}$ is given in (A.15). Since the thermal emission term includes powers of optical depth, we must also account for changes εv_q in optical depths in and below the layer q. Defining

$$I'^{(te)}_{jp} = I^{(te)}_{jp} + \varepsilon J^{(te)}_{jp}, \tag{B.26}$$

for the perturbed thermal emission particular integral, the following additional contributions are required in the eight boundary conditions of Section 3.3:

$$J^{(te)}_{jq} = \sum_{s=0}^{S} V_{jp,s}\tau^{s}_{q-1} \quad \text{for layer } q, \text{ upper boundary}, \tag{B.27a}$$

$$J^{(te)}_{jq} = \sum_{s=0}^{S} V_{jp,s}\tau^{s}_{q} + v_q \sum_{s=0}^{S} sT_{jq,s}\tau^{s-1}_{q} \quad \text{for layer } q, \text{ lower boundary}, \tag{B.27b}$$

$$J^{(te)}_{jp} = v_q \sum_{s=0}^{S} sT_{jp,s}\tau^{s-1}_{p} \quad \text{for layers } p > q, \text{ lower boundaries}. \tag{B.27c}$$

Eq. (B.27a) is required for BCL3, (B.27b) and (B.27c) for BCL4, and (B.27c) for BCL5 and BCL6. For BCL4M, (B.27b) is relevant for the thermal emission contribution to the positive (upwelling) quadrature-angle intensity components, but the downwelling stream components of the thermal emission contributions in (B.27b) must be integrated over the half-space and included in the surface reflection boundary condition.

B.11. Boundary condition BCL6R for albedo weighting functions

Layer homogeneous and particular solutions are unaffected by variations of the surface albedo, so we may use their unperturbed forms. Only the boundary value constants of integration will change, and we denote their first-order perturbations by $N^{(R)}_{q\alpha}$ and $P^{(R)}_{q\alpha}$ to indicate the dependence on albedo. The perturbed intensity in all layers will have the form expressed in (42b), with boundary condition BCL1 applying to the TOA level and BCL2 to all intermediate levels. To express the surface boundary condition for the perturbed field, we first rewrite the *unperturbed* reflecting

boundary condition in order to define $Q_j^{(R)}$ as follows (omitting the surface emission term):

$$I_{jK} \equiv RQ_j^{(R)} = R\left\{\frac{F_\odot \mu_0}{\pi}\rho^*(\mu_j, -\mu_0)\mathrm{e}^{-\tau_K/\mu_0} + (1+\delta_{m0})\sum_{i=1}^{N} a_i\mu_i\rho^*(\mu_j, -\mu_i)I_{-iK}\right\}. \tag{B.28}$$

For a variation $R' = R(1+\varepsilon)$, the perturbed version of (B.28) is

$$I'_{jK} = R(1+\varepsilon)\left\{\frac{F_\odot \mu_0}{\pi}\rho^*(\mu_j, -\mu_0)\mathrm{e}^{-\tau_K/\mu_0} + (1+\delta_{m0})\sum_{i=1}^{N} a_i\mu_i\rho^*(\mu_j, -\mu_i)I'_{-iK}\right\}, \tag{B.29}$$

where the perturbed downwelling quadrature-stream intensity at the surface is given by

$$I'_{-iK} = I_{-iK} + \varepsilon\sum_{\alpha=1}^{N}\{N_{K\alpha}^{(R)}\Theta_{K\alpha}X^+_{-iK\alpha} + P_{K\alpha}^{(R)}X^-_{-iK\alpha}\}. \tag{B.30}$$

Using BC3 to remove the zero-order terms, the special albedo boundary condition (BCL6R) for $j = 1, \ldots, N$ then becomes

$$\sum_{\alpha=1}^{N}[N_{K\alpha}^{(R)}\Theta_{K\alpha}\Phi^+_{j\alpha} + P_{K\alpha}^{(R)}\Phi^-_{j\alpha}] = U_j^{(6R)} \quad \text{(BCL6R)}, \tag{B.31}$$

where $U_j^{(6R)} = RQ_j^{(R)}$, and $\Phi^\pm_{j\alpha}$ have been defined in (35a). The solution for $N_{q\alpha}^{(R)}$ and $P_{q\alpha}^{(R)}$ again follows from the back-substitution $\mathscr{X}^{(R)} = \mathscr{A}^{-1}\mathscr{B}^{(R)}$, where $\mathscr{B}^{(R)}$ is now constructed from a combination of vectors $U^{(1)}$, $U_q^{(2)}$ and $U^{(6R)}$.

Appendix C. Post-processing (source function integration)

C.1. Source function integration for the original (unperturbed) field

Referring to the recurrence relation for the upwelling post-processed solution in Section 2.3 we substitute the values of $J_p(\tau, \mu)$ as given in (38) in the source function integration (37). Omitting the thermal emission term for now, the optical depth integrations may be carried out explicitly. The result for Λ_p is

$$\Lambda_p(\mu) = H_p(\mu)F_p(\mu) + \sum_{\alpha=1}^{N}[L_{p\alpha}G^+_{p\alpha}E^+_{p\alpha}(\mu) + M_{p\alpha}G^-_{p\alpha}E^-_{p\alpha}(\mu)], \tag{C.1}$$

where

$$E^+_{p\alpha}(\mu) = [1 - \Theta_{p\alpha}\gamma_p(\mu)]/(1+\mu k_{p\alpha}), \tag{C.2a}$$

$$E^-_{p\alpha}(\mu) = [\Theta_{p\alpha} - \gamma_p(\mu)]/(1-\mu k_{p\alpha}), \tag{C.2b}$$

$$F_p(\mu) = \mathrm{e}^{-\tau_{p-1}/\mu_0}[1 - \mathrm{e}^{-\Delta_p/\mu_0}\gamma_p(\mu)]/(1+\mu/\mu_0) \tag{C.2c}$$

and the transmittance factors $\Theta_{p\alpha}$ and $\gamma_p(\mu)$ have been defined previously. In addition, Eq. (C.1) requires the following double quadrature sums over discrete ordinate variables:

$$G^{\pm}_{p\alpha}(\mu) = \sum_j a_j D_p(\mu, \mu_j) X^{\pm}_{jp\alpha}, \tag{C.3a}$$

$$H_p(\mu) = \frac{F_\odot}{2\pi}(2 - \delta_{m0}) D_p(\mu, -\mu_0) + \sum_j a_j D_p(\mu, \mu_j) W_{jp}. \tag{C.3b}$$

Here D_p are the usual Legendre polynomial sums for the streams indicated, with single-scatter albedo and phase function moments defined for layer p. The quantities in (C.2) and (C.3) will be needed again when we carry out a perturbation analysis of (C.1).

For the inclusion of atmospheric thermal emission terms, there is an additional contribution $\Lambda^{(te)}_p(\mu)$ to the integrated layer source function in a given layer p. This is only present for Fourier component $m = 0$. In the source function integration, we must include the thermal emission particular integral given by the last term in (31). By analogy to (C.1) we define

$$\Lambda^{(te)}_p(\mu) = \sum_{s=0}^{S} U_{ps}(\mu) A_{ps}(\mu), \tag{C.4}$$

where the $A_{ps}(\mu)$ term arises from the optical depth integration, and the $U_{ps}(\mu)$ is a quadrature sum over discrete ordinate variables. It may be shown readily that

$$A_{ps}(\mu, \tau) = \begin{cases} 1 - \gamma_p(\mu) & \text{if } s = 0, \\ \tau_p^s - \tau_{p-1}^s \gamma_p(\mu) + s\mu A_{p,s-1}(\mu) & \text{if } s > 0 \end{cases} \tag{C.5a}$$

and

$$U_{ps}(\mu) = (1 - \omega_p) b_s + \sum_j a_j D_p(\mu, \mu_j) T_{jp,s}. \tag{C.5b}$$

The Legendre sum for layer D_p is defined in the usual way, using Fourier component $m = 0$.

It remains to find the boundary source term $I_K(\tau_K, \mu)$ which is the upwelling radiation at the lower boundary for direction μ. The discrete ordinate approximation is used again to write the reflection condition for direction μ in a similar manner to that given in (32c) and (33):

$$I_K(\tau_K, \mu) = (1 + \delta_{m0}) R \sum_{i=1}^{N} a_i \mu_i \rho^*_m(\mu, -\mu_i) I_{-iK}(\tau_K) + \frac{\mu_0 F_\odot}{\pi} e^{-\tau_K/\mu_0} R \rho^*_m(\mu, -\mu_0). \tag{C.6}$$

This is easy to evaluate since the components $I_{-iK}(\tau_K)$ are known from the discrete ordinate solution for the lowest layer K. It is necessary however to specify the bi-directional reflection functions $\rho^*_m(\mu, -\mu_i)$ and $\rho^*_m(\mu, -\mu_0)$ for the (user-defined) directions μ. (With surface thermal emission present, we add the factor $\delta_{m0}\kappa(\mu)B(T_g)$ to the right-hand side of (C.6), where the emissivity $\kappa(\mu)$ follows from (21)).

C.2. Source function integration for the perturbed field

In this section the same technique is applied to the perturbed intensity field. First we look at the source function integrations required for weighting functions with respect to layer variations, before dealing with the albedo weighting function source terms at the end.

For the layer variations, we require the perturbed form (44) for the source function recurrence relation, and we now consider the analysis for the perturbed source term $\Lambda'_p(\mu)$. Leaving aside the layer thermal emission terms for now (we return to them later in this section), we define perturbations of the quantities defined in (C.2) and (C.3):

$$E'^{\pm}_{p\alpha}(\mu) = E^{\pm}_{p\alpha}(\mu) + \varepsilon \mathscr{E}^{\pm}_{p\alpha}(\mu), \tag{C.7a}$$

$$F'_p(\mu) = F_p(\mu) + \varepsilon \mathscr{F}_p(\mu), \tag{C.7b}$$

$$G'^{\pm}_{q\alpha}(\mu) = G^{\pm}_{q\alpha}(\mu) + \varepsilon \mathscr{G}^{\pm}_{q\alpha}(\mu), \tag{C.7c}$$

$$H'_q(\mu) = H_q(\mu) + \varepsilon \mathscr{H}_q(\mu). \tag{C.7d}$$

For layer q, perturbations in (C.7a) and (C.7b) will depend both on terms εv_q induced in the optical depth boundary value τ_q, and on terms εu_q which will be manifested in the perturbed eigenvalues $k'_{q\alpha}$. For layers $p > q$, only variations v_q induced in the optical depth boundary values τ_p will be required. The results for $\mathscr{E}$ are

$$\mathscr{E}^{+}_{q\alpha} = \frac{\Theta_{q\alpha}\gamma_q(\mu)[\mu^{-1}v_q + \varpi_{q\alpha}] - \mu u_q f_{q\alpha} E^{+}_{q\alpha}(\mu)}{1 + \mu k_{q\alpha}}, \tag{C.8a}$$

$$\mathscr{E}^{-}_{q\alpha} = \frac{-\Theta_{q\alpha}\varpi_{q\alpha} + \mu^{-1}v_q\gamma_q(\mu) + \mu u_q f_{q\alpha} E^{-}_{q\alpha}(\mu)}{1 - \mu k_{q\alpha}}, \tag{C.8b}$$

$$\mathscr{E}^{\pm}_{p\alpha} = 0 \quad \text{for } p \neq q. \tag{C.8c}$$

In these equations, we use the following perturbation results on transmittance factors $\Theta_{q\alpha}$ and $\gamma_q(\mu)$:

$$\Theta'_{q\alpha} = \Theta_{q\alpha}(1 - \varpi_{q\alpha}\varepsilon), \tag{C.9a}$$

$$\gamma'_q(\mu) = \gamma_q(\mu)(1 - \varepsilon v_q/\mu), \tag{C.9b}$$

where $\varpi_{q\alpha}$ is given by (B.7). Similarly for $\mathscr{F}_p$ we have

$$\mathscr{F}_p = \begin{cases} v_q\mu^{-1}\mathrm{e}^{-\tau_q/\mu_0}\gamma_q(\mu) & \text{for } p = q, \\ -v_q\mu_0^{-1}F_p & \text{for } p > q, \\ 0 & \text{for } p < q. \end{cases} \tag{C.10}$$

Now consider the perturbation analysis for quantities G and H in (C.3a) and (C.3b), using the definitions in (C.7c) and (C.7d). As before, the quantities D_q perturb to first order with factor $(1 + \varepsilon u_q)$, since they are both directly proportional to ω_q. Using perturbations of the homogeneous solution vectors $X_{q\alpha}$ and the particular integral vectors W_q, we obtain

$$\mathscr{G}^{\pm}_{q\alpha}(\mu) = u_q\left[\sum_j a_j D_q(\mu,\mu_j)(X^{\pm}_{jq\alpha} + Y^{\pm}_{jq\alpha})\right], \tag{C.11a}$$

$$\mathscr{H}_q(\mu) = u_q\left[\frac{F_\odot}{2\pi}(2 - \delta_{m0})D_q(\mu,-\mu_0) + \sum_j a_j D_q(\mu,\mu_j)(W_{jq} + Z_{jq})\right]. \tag{C.11b}$$

It is clear that $\mathscr{G}^{\pm}_{p\alpha}(\mu)$ and $\mathscr{H}_p(\mu)$ are both zero for $p \neq q$.

We return now to the complete source function term in (C.1). This contains the integration constants $L_{p\alpha}$ and $M_{p\alpha}$. We must include their perturbations $N_{p\alpha}$ and $P_{p\alpha}$ in the analysis. We combine the results in (C.8), (C.10) and (C.11) and proceed by using the chain rule. The final result for the first-order layer source term perturbation is

$$\Lambda'_p(\mu) = \Lambda_p(\mu) + \varepsilon\Omega_p(\mu), \tag{C.12}$$

where (simplifying the notation by dropping the dependence on μ):

$$\Omega_p = \begin{cases} \sum_{\alpha=1}^{N} \Omega_{p\alpha}^{(1)} & \text{for } p < q, \\ \sum_{\alpha=1}^{N} [\Omega_{p\alpha}^{(1)} + \Omega_{p\alpha}^{(2)}] + H_p \mathscr{F}_p + \mathscr{H}_p F_p & \text{for } p = q, \\ \sum_{\alpha=1}^{N} \Omega_{p\alpha}^{(1)} + H_p \mathscr{F}_p & \text{for } p > q. \end{cases} \tag{C.13}$$

The following definitions are required:

$$\begin{aligned} \Omega_{p\alpha}^{(1)} &= N_{p\alpha} G_{p\alpha}^{+} E_{p\alpha}^{+} + P_{p\alpha} G_{p\alpha}^{-} E_{p\alpha}^{-}, \\ \Omega_{p\alpha}^{(2)} &= L_{p\alpha}[G_{p\alpha}^{+} \mathscr{E}_{p\alpha}^{+} + \mathscr{G}_{p\alpha}^{+} E_{p\alpha}^{+}] + M_{p\alpha}[G_{p\alpha}^{-} \mathscr{E}_{p\alpha}^{-} + \mathscr{G}_{p\alpha}^{-} E_{p\alpha}^{-}]. \end{aligned} \tag{C.14}$$

We now consider perturbations of the thermal emission layer source terms defined in (C.4). These contributions will be added to the above expressions for Ω_p when there is a thermal emission source present in the atmosphere. First, we note that the solution coefficients U_{ps} contain no dependence on optical depth, so they experience perturbation only for the layer q that contains the atmospheric parameter x_q causing the variation. Defining

$$U'_{qs}(\mu) = U_{qs}(\mu) + \varepsilon \mathscr{U}_{qs}(\mu), \tag{C.15}$$

we find from the definitions in (C.5b) that

$$\mathscr{U}_{qs}(\mu) = [(1 - \omega_q)h_{qs} - u_q \omega_q b_{qs}] + \sum_j a_j D_q(\mu, \mu_j)(u_q T_{jq,s} + V_{jq,s}), \tag{C.16}$$

where h_{qs} are the perturbations of b_{qs}. The recurrence factors A_{ps} in (C.5a) are perturbed as follows:

$$A'_{ps}(\mu) = A_{ps}(\mu) + \varepsilon B_{ps}(\mu). \tag{C.17}$$

We must again distinguish between the layer q containing the parameter x_q, and layers below q. Values of B_{ps} are found to obey similar recurrence relationships to those for A_{ps}. The result is

$$B_{ps}(\mu) = \begin{cases} 0 & \text{for } p < q, \quad s = 0, \ldots, S, \\ v_q r_q(\mu)/\mu & \text{for } p = q, \quad s = 0, \\ v_q \tau_q^s \gamma_q(\mu)\left(\dfrac{1}{\mu} + \dfrac{s}{\tau_q}\right) + s\mu B_{q,s-1}(\mu) & \text{for } p = q, \quad s = 1, \ldots, S, \\ 0 & \text{for } p > q, \quad s = 0, \\ s v_q(\tau_p^{s-1} - \tau_{p-1}^{s-1}\gamma_p(\mu)) + s\mu B_{p,s-1}(\mu) & \text{for } p > q, \quad s = 1, \ldots, S. \end{cases} \tag{C.18}$$

For the perturbation of the thermal emission contribution to the source integral term, we write

$$\Lambda'^{(\mathrm{te})}_p(\mu) = \Lambda^{(\mathrm{te})}_p(\mu) + \varepsilon\Omega^{(\mathrm{te})}_p(\mu) \tag{C.19}$$

and use the above results in (C.16) and (C.18) to produce

$$\Omega_p^{(\mathrm{te})}(\mu) = \begin{cases} \sum_{s=0}^{S} [U_{ps}(\mu) B_{ps}(\mu) + \mathscr{U}_{ps}(\mu) A_{ps}(\mu)] & \text{for } p = q, \\ \sum_{s=0}^{S} U_{ps}(\mu) B_{ps}(\mu) & \text{for } p > q, \end{cases} \tag{C.20}$$

with $\Omega_p^{(\mathrm{te})}(\mu) = 0$ for $p < q$. These contributions should be added to those in (C.12) so that thermal emission terms can be included in the TOA weighting functions at arbitrary μ.

Now we examine the perturbation of the upwelling lower boundary source term $I_K(\tau_K,\mu)$ in (C.6). We use the definition

$$I'_K(\tau_K, \mu) = I_K(\tau_K, \mu) + \varepsilon J_K(\tau_K, \mu) \tag{C.21}$$

and our task is to determine $J_K(\tau_K, \mu)$. Since the perturbed field obeys the surface boundary condition, we can remove the zero-order terms (boundary condition BC3) and write the following for the first-order contribution:

$$J_K(\tau_K, \mu) = (1 + \delta_{m0}) R \sum_{i=1}^{N} a_i \mu_i \rho_m^*(\mu, -\mu_i) J_K(\tau_K, -\mu_i) - \frac{v_q}{\mu_0} I^*(\mu), \tag{C.22}$$

where the last term is the variation of the direct-beam term $I^*(\mu)$ as given by Eq. (33) minus the surface emission, and $J_K(\tau_K, -\mu_j)$ is the first-order perturbation for the downwelling radiation at the *quadrature* values. In other words, $I'_K(\tau_K, -\mu_j) = I_K(\tau_K, -\mu_j) + \varepsilon J_K(\tau_K, -\mu_j)$. Expressions for $J_K(\tau_K, -\mu_j)$ can be written down immediately, since the results are available from the boundary problem perturbation analysis. There are two cases: BCL6, for which $q < K$, and BCL4M, for which $q = K$:

$$J(\tau_K, -\mu_j) = \begin{cases} -\dfrac{v_q W_{-jK}}{\mu_0} \mathrm{e}^{-\tau_K/\mu} + \displaystyle\sum_{\alpha=1}^{N} [N_{K\alpha} \Theta_{K\alpha} X^+_{-jK\alpha} + P_{K\alpha} X^-_{-jK\alpha}] & \text{(BCL6)}, \\ \left(u_q Z_{-jq} - \dfrac{v_q W_{-jq}}{\mu_0} \right) \mathrm{e}^{-\tau_q/\mu} + \displaystyle\sum_{\alpha=1}^{N} \{ P_{q\alpha} X^-_{-jq\alpha} + M_{q\alpha} u_q Y^-_{-jq\alpha} \} & \\ \quad + \displaystyle\sum_{\alpha=1}^{N} \Theta_{q\alpha} \{ N_{q\alpha} X^+_{-jq\alpha} + L_{q\alpha} [u_q Y^+_{-jq\alpha} - X^+_{-jq\alpha} \varpi_{q\alpha}] \} & \text{(BCL4M)}. \end{cases} \tag{C.23}$$

C.3. Albedo weighting functions at arbitrary μ

We complete this appendix by examining the perturbed field at arbitrary μ for an albedo variation. Homogeneous and particular solutions remain unchanged, and only the constants of integration in the boundary-value problem will be perturbed. We proceed using definition (C.12), writing $\Omega_p^{(R)}(\mu)$ for the source function perturbation, where the superscript (R) is used to indicate quantities derived with respect to an albedo variation $R' = R(1 + \varepsilon)$. We find

$$\Omega_p^{(R)}(\mu) = \sum_{\alpha=1}^{N} [N_{p\alpha}^{(R)} G_{p\alpha}^+ E_{p\alpha}^+ + P_{p\alpha}^{(R)} G_{p\alpha}^- E_{p\alpha}^-] \quad \text{for all } p, \tag{C.24}$$

where all other quantities occur in the original unperturbed solution.

To start the source function recurrence, we need the perturbed upwelling intensity at the lower boundary. To first order, we define $I'_K(\tau_K,\mu) = I_K(\tau_K,\mu) + \varepsilon J_K^{(R)}(\tau_K,\mu)$. Ignoring the surface emission term, we apply the surface boundary condition to $I'_K(\tau_K,\mu)$ and obtain

$$J_K^{(R)}(\tau_K,\mu) = (1+\delta_{m0})R\sum_{i=1}^{N} a_i\mu_i\rho_m^*(\mu,-\mu_i)[I_K(\tau_K,-\mu_i) + J_K^{(R)}(\tau_K,-\mu_i)] + I^*(\mu), \tag{C.25}$$

where $I^*(\mu)$ has already been defined in (33). From the solution of the perturbed albedo boundary value problem, we have already the quadrature terms:

$$J_K^{(R)}(\tau_K,-\mu_j) = \sum_{\alpha=1}^{N} [N_{K\alpha}^{(R)}\Theta_{K\alpha}X^+_{-jK\alpha} + P_{K\alpha}^{(R)}X^-_{-jK\alpha}]. \tag{C.26}$$

Appendix D. Chandrasekhar's solution and associated perturbation analysis

We first derive Chandrasekhar's solution to the unperturbed RTE. The notation follows that in [12]; in particular the Legendre polynomials in this appendix are un-normalized. The Fourier index m is retained throughout. Quadrature over the interval $\mu\in(-1,1)$ is assumed. The treatment of thermal emission is omitted.

For the homogeneous part, Chandrasekhar developed solutions of the form

$$I^m(\mu_i) \sim \sum_{l=m}^{2N-1} \frac{\xi_l^m(k_\alpha^m)\varphi_l^m P_l^m(\mu_i)}{1+\mu_i k_\alpha^m} \mathrm{e}^{-k_\alpha^m\tau}, \tag{D.1}$$

where μ_i are the quadrature cosines, k_α^m are the roots of the characteristic equation (see below), and factors ξ_l^m are to be determined (their dependence on k_α^m is indicated). Here, $\varphi_l^m = \beta_l(l-m)!/(l+m)!$ denotes the phase moment factorial term. Substitution of Eq. (D.1) in the RTE (15) without the external source terms gives the following set of conditions for $\xi_l^m(k)$:

$$\xi_l^m(k) = \sum_{\lambda=m}^{2N-1} \xi_\lambda^m(k)\varphi_\lambda^m D_{l\lambda}^m(k), \tag{D.2}$$

where

$$D_{l\lambda}^m(k) = \frac{1}{2}\sum_j \frac{a_j P_\lambda^m(\mu_j)P_l^m(\mu_j)}{1+\mu_j k}. \tag{D.3}$$

Using the orthonormality of the Legendre polynomials over the interval $(-1,1)$, one can develop a recurrence relation for the D-polynomials in (D.3), and use that to generate further recurrence relations for ξ_l^m ([12, p. 153]):

$$\xi_{l+1}^m(k) = \frac{-(2l+1)+\omega\beta_l}{k(l-m+1)}\xi_l^m(k) - \frac{l+m}{l-m+1}\xi_{l-1}^m(k) \quad \text{for } m+1<l<2N-2, \tag{D.4a}$$

$$\xi_{m+1}^m(k) = \frac{-(2m+1)+\omega\beta_m}{k}. \tag{D.4b}$$

The indeterminacy in (D.2) allows the recursion initialization condition to be set at will. Letting $\xi_m^m = 1$ gives the characteristic equation

$$1 = \frac{\omega}{2}\sum_j \frac{a_j}{1+\mu_j k} \sum_{\lambda=m}^{2N-1} \xi_\lambda^m(k)\varphi_\lambda^m P_\lambda^m(\mu_j) P_m^m(\mu_j). \tag{D.5}$$

The roots of (D.5) occur in pairs $\pm k_\alpha$, $\alpha = 1, \ldots, N$. It is no surprise that these roots are precisely the eigenvalues from the equivalent formulation in Eq. (22). We again use the index α to label the roots (eigenvalues). It is also clear that (up to constants of proportionality) the solutions developed in Section 2 are given by the following:

$$X_{j\alpha}^{m+} = \sum_{l=m}^{2N-1} \frac{\xi_l^m(k_\alpha^m)\varphi_l^m P_l^m(\mu_j)}{1+\mu_j k_\alpha^m}, \tag{D.6a}$$

$$X_{j\alpha}^{m-} = \sum_{l=m}^{2N-1} \frac{\xi_l^m(-k_\alpha^m)\varphi_l^m P_l^m(\mu_j)}{1-\mu_j k_\alpha^m}. \tag{D.6b}$$

For the particular integral (beam source), a solution of the form

$$J^m(\mu_i) = (2-\delta_{m0}) W_i^m \mathrm{e}^{-\tau/\mu_0} \tag{D.7}$$

is used, where

$$W_i^m = \omega \sum_{l=m}^{2N-1} \frac{\gamma_l^m \varphi_l^m P_l^m(\mu_i)}{1+\mu_i/\mu_0}. \tag{D.8}$$

Substitution in the RTE yields the following equation for the constants γ_l^m in terms of the recurrence factors defined above:

$$\gamma_l^m = \gamma_m^m(\mu_0)\xi_l^m(\mu_0^{-1}) \quad \text{for } l > m, \tag{D.9a}$$

$$\gamma_m^m(\mu_0) = \frac{P_m^m(\mu_0)}{1 - \sum_{\lambda=m}^{2N-1} \xi_\lambda^m(\mu_0^{-1})\varphi_\lambda^m D_{m\lambda}^m(\mu_0^{-1})}, \tag{D.9b}$$

where ξ_l^m are again given by the recurrence relation Eqs. (D.4a) and (D.4b) but with argument μ_0^{-1} instead of k. Symmetry relationships are the same as those for the solutions in Section 2.2.

This formulation is equivalent to the solution of the RTE given in Section 2.2, assuming the "single" quadrature scheme (numerical results agree to high accuracy). This analytic formalism is not valid for the "double" quadrature scheme. Clearly, all quantities can be computed explicitly once the roots of the characteristic equation are found. Attempts to evaluate these roots by polynomial root-finding algorithms [37] have now been supplanted by the eigenvalue approach.

D.1. Perturbation of the solution

We are interested only in the perturbation of the RTE homogeneous solutions and particular integrals. (The boundary condition analysis of Section 3.3 is independent of the method of

obtaining RTE solutions). The definitions of (40a)–(40c) hold, but we suppress the layer index p and add the Fourier harmonic index m as a subscript:

$$k_\alpha'^m = k_\alpha^m + u\varepsilon f_\alpha^m, \qquad X_{j\alpha}'^m = X_{j\alpha}^m + u\varepsilon Y_{j\alpha}^m \quad \text{and} \quad W_j'^m = W_j^m + u\varepsilon Z_j^m. \tag{D.10}$$

As in Section 3, the single-scatter albedo will be perturbed according to $\omega' = \omega(1 + u\varepsilon)$. We perturb the recurrence relation (D.4a) and (D.4b) first. We write $\xi_{l,\alpha}^m = \xi_l^m(k_\alpha^m)$ for the quantity ξ corresponding to root k_α^m, and for the first-order perturbation, we define

$$\xi_{l,\alpha}'^m = \xi_{l,\alpha}^m + u\varepsilon(\zeta_{l,\alpha}^m + \eta_{l,\alpha}^m f_\alpha^m). \tag{D.11}$$

Using the perturbation rules for ω and k_α^m, and equating terms in u and uf_α^m, we find that $\zeta_{l,\alpha}^m$ and $\eta_{l,\alpha}^m$ satisfy recurrence relationships similar to Eqs. (D.4a) and (D.4b), but with additional terms

$$\zeta_{l+1,\alpha}^m = \frac{\omega\beta_l}{k_\alpha^m(l-m+1)}\xi_{l,\alpha}^m + \frac{-(2l+1)+\omega\beta_l}{k_\alpha^m(l-m+1)}\zeta_{l,\alpha}^m - \frac{l+m}{l-m+1}\zeta_{l-1,\alpha}^m, \tag{D.12a}$$

$$\eta_{l+1,\alpha}^m = \frac{(2l+1)-\omega\beta_l}{(k_\alpha^m)^2(l-m+1)}\xi_{l,\alpha}^m + \frac{-(2l+1)+\omega\beta_l}{k_\alpha^m(l-m+1)}\eta_{l,\alpha}^m - \frac{l+m}{l-m+1}\eta_{l-1,\alpha}^m, \tag{D.12b}$$

$$\zeta_{m+1,\alpha}^m = \frac{\omega\beta_m}{k_\alpha^m}, \tag{D.12c}$$

$$\eta_{m+1,\alpha}^m = \frac{(2l+1)-\omega\beta_m}{(k_\alpha^m)^2}. \tag{D.12d}$$

Eqs. (D.12a) and (D.12b) are valid for $m+1 < l < 2N-2$. The starting points for these recurrences are $\xi_{m,\alpha}^m = 0$ and $\eta_{m,\alpha}^m = 0$. We now substitute (D.11), (D.12a)–(D.12d) and definitions (D.10) into the perturbed version of the characteristic equation (D.5) to obtain variations for k_α^m:

$$f_\alpha^m = \frac{\Psi_\alpha^m + 2/\omega}{\Lambda_\alpha^m - \Phi_\alpha^m}, \tag{D.13}$$

where

$$\Psi_\alpha^m = \sum_j \frac{a_j}{(1+\mu_j k_\alpha^m)^2}\left\{\sum_{\lambda=m}^{2N-1} \zeta_{\lambda,\alpha}^m \varphi_\lambda^m P_\lambda^m(\mu_j) P_m^m(\mu_j)\right\}, \tag{D.14a}$$

$$\Lambda_\alpha^m = \sum_j \frac{\mu_j a_j}{(1+\mu_j k_\alpha^m)^2}\left\{\sum_{\lambda=m}^{2N-1} \xi_{\lambda,\alpha}^m \varphi_\lambda^m P_\lambda^m(\mu_j) P_m^m(\mu_j)\right\} \tag{D.14b}$$

and

$$\Phi_\alpha^m = \sum_j \frac{a_j}{(1+\mu_j k_\alpha^m)^2}\left\{\sum_{\lambda=m}^{2N-1} \eta_{\lambda,\alpha}^m \varphi_\lambda^m P_\lambda^m(\mu_j) P_m^m(\mu_j)\right\}. \tag{D.14c}$$

Eq. (D.13) may be compared directly to the results obtained for quantity f_α in Appendix A. To find the perturbed solution vector $X_\alpha'^{m+}$, we define a perturbed form of (D.6a):

$$X_{j\alpha}'^{m+} = X_{j\alpha}^{m+} + \varepsilon u Y_{j\alpha}^{m+} = \sum_{l=m}^{2N-1} \frac{\xi_l'^m(k_\alpha'^m)\varphi_l^m P_l^m(\mu_j)}{1+\mu_j k_\alpha'^m}. \tag{D.15}$$

Using the definitions in Eq. (D.10) and the results in Eqs. (D.12a)–(D.12d), (D.13) and (D.14a)–(D.14c), we find after some manipulation that the perturbation factor $Y_{j\alpha}^{m+}$ is given by

$$Y_{j\alpha}^{m+} = \sum_{l=m}^{2N-1} \frac{\omega\varphi_l^m P_l^m(\mu_j)}{1+\mu_j k_\alpha^m}\left\{\xi_{l,\alpha}^m + \zeta_{l,\alpha}^m + f_\alpha^m\left(\eta_{l,\alpha}^m - \frac{\xi_{l,\alpha}^m \mu_j}{1+\mu_j k_\alpha^m}\right)\right\}. \tag{D.16}$$

Perturbations for the negative solution (D.6b) can be determined in a similar fashion.

For the particular integral (beam source), look first at the perturbation:

$$\xi_{l,\alpha}'^m(\mu_0^{-1}) = \xi_{l,\alpha}^m(\mu_0^{-1}) + u\varepsilon\zeta_{l,\alpha}^m(\mu_0^{-1}). \tag{D.17}$$

This time only the variation in ω is required, and since ξ satisfies the recurrence relations (D.4a) and (D.4b) with μ_0^{-1} instead of k, then ζ in (D.17) will satisfy a similar recurrence with additional terms:

$$\zeta_{l+1}^m = \frac{\omega\beta_l}{l-m+1}\mu_0\xi_l^m + \frac{-(2l+1)+\omega\beta_l}{l-m+1}\mu_0\zeta_l^m - \frac{l+m}{l-m+1}\zeta_{l-1}^m$$

$$\text{for } m+1 < l < 2N-2, \tag{D.18a}$$

$$\zeta_{m+1}^m = \mu_0\omega\beta_m. \tag{D.18b}$$

The recurrence (D.18a) and (D.18b) starts with $\zeta_m^m = 0$. This result is now used in the perturbation of the γ_l^m constants in (D.9a) and (D.9b). Defining

$$W_i'^m = W_i^m + \varepsilon u Z_i^m = \omega' \sum_{l=m}^{2N-1} \frac{\gamma_l'^m \varphi_l^m P_l^m(\mu_i)}{1+\mu_i/\mu_0}, \tag{D.19}$$

where

$$\gamma'^m_l = \gamma_l^m(1+\varepsilon u\Gamma_l^m), \tag{D.20}$$

then we find after manipulation that

$$Z_i^m = \omega \sum_{l=m}^{2N-1} \frac{\gamma_l^m\varphi_l^m(1+\Gamma_l^m)P_l^m(\mu_i)}{1+\mu_i/\mu_0}, \tag{D.21}$$

where

$$\Gamma_l^m = \frac{\zeta_l^m}{\xi_l^m} - \frac{\omega\sum_{\lambda=m}^{2N-1}(\xi_\lambda^m+\zeta_\lambda^m)\varphi_\lambda^m D_{m\lambda}^m}{1-\sum_{\lambda=m}^{2N-1}\xi_\lambda^m\varphi_\lambda^m D_{m\lambda}^m}. \tag{D.22}$$

This completes the analytic perturbation for the beam solution.

References

[1] Marquardt DW. J Soc Ind Appl Math 1963;11:431.
[2] Carlotti M. Global-fit approach to the analysis of limb-scanning atmospheric measurements. Appl Opt 1988;27:3250–4.
[3] Rodgers CD. Retrieval of atmospheric temperature and composition from remote measurements of thermal radiation. Rev Geophys Space Phys 1976;14:609–24.

[4] Rodgers CD. Characterization and error analysis of profiles retrieved from remote sounding experiments. J Geophys Res 1990;95:5587.
[5] Bhartia PK, McPeters RD, Mateer CL, Flynn LE, Wellemeyer C. Algorithm for the estimation of vertical ozone profiles from the backscattered ultraviolet technique. J Geophys Res 1996;101:18793–806.
[6] Chance K, Burrows JP, Perner D, Schneider W. Satellite measurements of atmospheric ozone profiles, including tropospheric ozone, from UV/visible measurements in the nadir geometry: a potential method to retrieve tropospheric ozone. JQSRT 1997;57:467–76.
[7] Munro R, Siddans R, Reburn WJ, Kerridge BJ. Direct measurement of tropospheric ozone distributions from space. Nature 1998;392:168–71.
[8] Hoogen R, Rozanov V, Burrows J. Ozone profiles from GOME satellite data: algorithm description and first validation. J Geophys Res 1999;104:8263–80.
[9] Engl HW, Hanke M, Neubauer A. Regularization of inverse problems In: Mathematics and its applications, vol. 375. Dordrecht: Kluwer Academic Publishers, 1996.
[10] Chu WP, McCormick M, Lenoble J, Brogniez C, Pruvost P. SAGE II inversion algorithm. J Geophys Res 1989;94:8339–51.
[11] Lenoble J editor. Radiative transfer in scattering and absorbing atmospheres. Hampton VA, USA: Deepak Publishing, 1985.
[12] Chandrasekhar S. Radiative transfer. New York: Dover Publications Inc., 1960.
[13] Chandrasekhar S. Selected papers, vol. 2. New York: University of Chicago Press, 1989.
[14] Stamnes K, Tsay S-C, Wiscombe W, Jayaweera K. Numerically stable algorithm for discrete ordinate method radiative transfer in multiple scattering and emitting layered media. Appl Opt 1988;27:2502–9.
[15] Berk MA, Bernstein LS, Robertson D. MODTRAN: a moderate resolution model for LOWTRAN7. Technical Report GL-TR-89-0122, Geophysics Laboratory, Hanscomb AFB, MA, 1989.
[16] ESA/ESTEC, Noordwijk, The Netherlands, GOME users manual, 1998.
[17] Rozanov V, Kurosu T, Burrows J. Retrieval of atmospheric constituents in the UV/visible: a new quasi-analytical approach for the calculation of weighting functions. JQSRT 1998;60:277–99.
[18] Barkstrom BR. A finite difference method of solving anisotropic scattering problems. JQSRT 1976;16: 725–39.
[19] Rozanov VV, Diebel D, Spurr RJD, Burrows JP. GOMETRAN: a radiative transfer model for the satellite project GOME - the plane parallel version. J Geophys Res 1997;102:16683–95.
[20] Thomas GE, Stamnes K. Radiative Transfer in the Atmosphere and Ocean, 1st ed. Cambridge: Cambridge University Press, 1999.
[21] Stamnes K, Swanson RA. A new look at the discrete ordinate method for radiative transfer in anisotropically scattering atmospheres. J Atmos Sci 1981;38:387–99.
[22] Dlugach JM, Yanovitskij EG. The optical properties of Venus and the Jovian planets. II. Methods and results of calculations of the intensity of radiation diffusely reflected from semi-infinite homogeneous atmospheres. Icarus 1974;22:66–81.
[23] Kurosu T, Rozanov VV, Burrows JP. Parameterization schemes for terrestrial water clouds in the radiative model GOMETRAN. J Geophys Res 1997;102:21809–23.
[24] Stamnes K, Conklin P. A new multi-layer discrete ordinate approach to radiative transfer in vertically inhomogeneous atmospheres. JQSRT 1984;31:273.
[25] Anderson E, Bai Z, Bischof C, Demmel J, Dongarra J, Du Croz J, Greenbaum A, Hammarling S, McKenney A, Ostrouchov S, Sorensen D. LAPACK User's guide, 2nd ed., Philadelphia: Society for Industrial and Applied Mathematics, 1995.
[26] Siewert CE. A concise and accurate solution to Chandrasekhar's basic problem in radiative transfer. JQSRT 2000;64:109–30.
[27] Press WH, Teukolsky SA, Vetterling WT, Flannery BP. Numerical recipes in Fortran 77, 2nd ed., Cambridge: Cambridge University Press, 1992.
[28] Goody RM, Yung YK. Atmospheric radiation, 2nd ed. Oxford: Oxford University Press, 1989.
[29] McClatchey R, Fenn RW, Selby JE, Volz FE, Garing JS. Optical properties of the atmosphere, AFCRL-TR-72-0497, Environmental Research Paper 411, 3rd ed. Bedford, MA: Air Force Cambridge Res Lab, 1972.

[30] Bass AM, Paur RJ. The UV cross-sections of ozone: 1. Measurements in atmospheric ozone. Proceedings of the Quadrennial Ozone Symposium, Halkidiki, Greece, 1985, p. 606–16.
[31] Chance K, Spurr RJD. Ring effect studies: Rayleigh scattering, including molecular parameters for rotational Raman scattering, and the Fraunhofer spectrum. Appl Opt 1997;36:5224–30.
[32] Shettle EP, Fenn RW. Models of the aerosols of the lower atmosphere and the effects of humidity variations on their optical properties. Technical Report AFGL-TR-79-0214, Geophysics Laboratory, Hanscomb AFB, MA 01732, 1979.
[33] Dahlback A, Stamnes K. A new spherical model for computing the radiation field available for photolysis and heating at twilight. Planet Space Sci 1991;39:671–83.
[34] Wiscombe WJ. The delta-M method: rapid yet accurate radiative flux calculations for strongly asymmetric phase functions. J Atmos Sci 1977;34:1408–22.
[35] Schulz FM, Stamnes K, Weng F. VDISORT: an improved and generalized discrete ordinate method for polarized (vector) radiative transfer. JQSRT 1999;61:105–22.
[36] Schulz FM, Stamnes K. Angular distribution of the Stokes vector in a plane-parallel vertically inhomogeneous medium in the vector discrete ordinate radiative transfer (VDISORT) model. JQSRT 2000;65:609–20.
[37] Liou KN. A numerical experiment on Chandrasekhar's discrete-ordinate method for radiative transfer: applications to cloudy and hazy atmospheres. J Atmos Sci 1973;30:1303.